ACADEMIA QUANTUM

Research Article
Published: 2025-10-21
https://doi.org/10.20935/ AcadQuant7957

Climbing the diagonal Clifford hierarchy

Jingzhen Hu[1,*] Qingzhong Liang[1], Robert Calderbank[1,2,3]

Academic Editor: Yuhua Duan

Abstract

Magic state distillation and the Shor factoring algorithm make essential use of logical diagonal gates. We introduce a method of synthesizing CSS codes that realize a target logical diagonal gate at some level l in the Clifford hierarchy. The method combines three basic operations: concatenation, removal of Z-stabilizers, and addition of X-stabilizers. It explicitly tracks the logical gate induced by a diagonal physical gate that preserves a CSS code. The first step is concatenation, where the input is a CSS code and a physical diagonal gate at level l inducing a logical diagonal gate at the same level. The output is a new code for which a physical diagonal gate at level $l+1$ induces the original logical gate. The next step is judicious removal of Z-stabilizers to increase the level of the induced logical operator. We identify three ways of climbing the logical Clifford hierarchy from level l to level $l+1$, each built on a recursive relation on the Pauli coefficients of the induced logical operators. Removal of Z-stabilizers may reduce distance, and the purpose of the third basic operation, addition of X-stabilizers, is to compensate for such losses. The approach to logical gate synthesis taken in prior work focuses on the code states, resulting in sufficient conditions for a CSS code to be fixed by a transversal Z-rotation. In contrast, we derive necessary and sufficient conditions by analyzing the action of a transversal diagonal gate on the stabilizer group that determines the code. The power of our approach to logical gate synthesis is demonstrated by two proofs of concept: the $[\![2^{l+1}-2,2,2]\!]$ triorthogonal code family and the $[\![2^m,\binom{m}{r},2^{\min\{r,m-r\}}]\!]$ quantum Reed–Muller code family.

Keywords: *quantum computing, quantum error correction, Calderbank-Shor-Steane (CSS) codes, diagonal quantum gates, coding theory, Clifford hierarchy, decoherence-free subspace*

Citation: Hu J, Liang Q, Calderbank R. Climbing the diagonal Clifford hierarchy. *Academia Quantum* 2025;2. https://doi.org/10.20935/ AcadQuant7957

1. Introduction

Quantum error correction provides a foundation for fault-tolerant quantum computation, enabling the protection of logical qubits from the pervasive noise affecting physical implementations. An $[\![n,k,d]\!]$ quantum error-correcting code (QECC) encodes k qubits of source information into n physical qubits such that the smallest undetectable error is on at least d (among the n) physical qubits. The stabilizer code framework [1–4] provides a method of correcting fewer than $d/2$ errors without compromising the encoded information by learning anything about it. There are many sources of error in quantum systems, including independent Pauli errors (bit-flip X, phase-flip Z) and errors under decoherence processes such as amplitude damping and dephasing induced by system-environment interactions [5]. In addition to these canonical errors, practical implementations contend with operational imperfections, including stochastic noise in quantum channels [6], coherent gate errors arising from systematic over-rotations [7], measurement misclassification due to imperfect detectors [8], and correlated errors such as qubit crosstalk [9]. The scalability of fault-tolerant quantum architectures depends on QECCs that are able to withstand the interaction of errors and imperfections.

The challenge of quantum computing is to combine error resilience with universal computation. While there are many ways to construct a universal gate set, a standard approach is to augment the set of Clifford gates by a non-Clifford unitary [10] such as the T gate $\left(T=Z^{1/4}\right)$. Gottesman and Chuang [11] defined the *Clifford hierarchy* when introducing the teleportation model of quantum computing. The first level is the *Pauli group*. The second level is the *Clifford group*, which consists of unitary operators that normalize the Pauli group. The l^{th} level consists of unitary operators that map Pauli operators to the $(l-1)^{\text{th}}$ level under conjugation. Section 2 introduces the Clifford hierarchy, which organizes unitary operators according to the way they commute with the Pauli group. The structure of the Clifford hierarchy has been studied extensively [12–19]. It is fundamental to quantum computation with connections to unitary designs and approximations [20, 21]. However, a full mathematical understanding of the Clifford hierarchy above the third level is lacking.

QECCs encode logical qubits into physical qubits and protect information as it is transformed by logical gates. In this work, we focus on diagonal operators in the Clifford hierarchy, in part because they are simple to implement. We start from a target diagonal logical operator, and we provide a general method for synthesizing a CSS code [1, 2] preserved by a diagonal physical gate that induces the target logical operator. Logical diagonal

[1]Department of Mathematics, Duke University, Durham, NC, USA.
[2]Department of Electrical and Computer Engineering, Duke University, Durham, NC, USA.
[3]Department of Computer Science, Duke University, Durham, NC, USA.
*email: journeyjingzhen@gmail.com

gates play a central role in quantum algorithms. In the Shor factoring algorithm [22, 23], our method applies to the $\mathrm{C}^{(i)}Z^{1/2^j}$ diagonal gates (see Section 2 for its definition), which play an essential role in period finding. In magic state distillation (MSD) [24–29], the effectiveness of the protocol depends on engineering the interaction of a diagonal physical gate with the code states of a stabilizer code [3, 4]. MSD motivates subsequent studies [30–37] on construction of $[\![n, k, d]\!]$ QECCs with low overhead exponent $\gamma = \frac{\log n/k}{\log d}$ that support transversal non-Clifford gates and on improvement of the distillation schemes. Our method transforms a CSS code supporting a lower-level logical operator to a CSS code supporting a higher-level logical operator. The coefficients in the Pauli expansion of a diagonal gate satisfy a recursion that makes it possible to work backwards from a target logical gate and tune the CSS code parameters.

Throughout the paper, we make use of an explicit representation of the logical channel induced by a diagonal physical gate. We prepare an initial state, apply a physical gate, then measure a code syndrome $\boldsymbol{\mu}$, and finally apply a correction based on $\boldsymbol{\mu}$. For each syndrome, we expand the induced logical operator in the Pauli basis to obtain the *generator coefficients* [38, 39] that capture state evolution. Intuitively, the diagonal physical gate preserves the code space if and only if the induced logical operator corresponding to the trivial syndrome is unitary. To support the objective of fault tolerance, we emphasize *transversal* gates [3], which are tensor products of unitaries on individual code blocks. The approach taken in prior work is to focus on the code states and to derive sufficient conditions for a stabilizer code to be fixed by a transversal Z-rotation [24–26, 28–31, 33, 40]. In contrast, we derive necessary and sufficient conditions by analyzing the action of a transversal diagonal gate on the stabilizer group that determines the code, generalizing the work on *CSS-T* code families [41–46]. Tracking the induced logical operator also provides mathematical insight into the Clifford hierarchy [19, 47] and informs circuit design [48].

As quantum computers transition from laboratory prototypes to fully programmable devices, researchers are increasingly focusing on coherent errors, and especially on the decay in coherence of the effective induced logical channel [49–51]. The action of a diagonal physical operator U_Z on code states depends sensitively on the signs of Z-stabilizers [52–55] and our generator coefficient framework captures how these signs change the logical operators induced by U_Z. For the coherent noise model [7], we demonstrate that a judicious choice of signs creates a decoherence-free subspace (DFS) [56–59], that enables data storage. The switch between computation and storage by applying a Pauli matrix is described in Remark 2. In experiments, Shival Dasu et al. [60] recently demonstrated on a trapped-ion device [61, 62] that a concatenated scheme, where the low-level code is a passively stable $[\![2, 1, 1]\!]$ repetition code (with a chosen stabilizer sign pattern to ensure DFS) and the high-level is a $[\![5, 1, 3]\!]$ code [63], extends memory times by over an order of magnitude.

To implement fault-tolerant quantum computation efficiently, several works focus on constructing QECCs with high encoding rates that support transversal non-Clifford gates. Haah [40] used divisibility properties of classical codes to construct CSS codes with parameters $[\![O(d^{l-1}), \Omega(d), d]\!]$ (In asymptotic analysis, $O(x)$ denotes an upper bound, meaning the growth rate of a function is at most proportional to x, while $\Omega(x)$ denotes a lower bound, meaning the growth rate is at least proportional to x.) that realize a transversal logical $Z^{1/2^{l-1}}$. Generalizing the work of Krishna and Tillich [32], Golowich and Guruswami [64] constructed $[\![n, k, d]\!]$ code families with k and d both growing linearly in the block length n that supports transversal Controlled-Controlled-Z gates. Jain and Albert [65] focused on the single logic qubit codes $[\![n, 1, d]\!]$ with high distance in which both Clifford gates and the T gate can be supported transversally. Vasmer and Kubica [66] introduced morphing procedures by exploring the possible routes from the stabilizer to its commutative subgroups, resulting in the $[\![n, k, d]\!]$ child code with fewer physical qubit n, the same logical qubits k, and possibly less distance d than its parent code. In contrast, we introduce three basic operations—concatenation, removal of Z-stabilizers, and addition of X-stabilizers—that can be combined to synthesize an arbitrary logical diagonal gate with more flexibility on the code parameters. We present the $[\![2^m, \binom{m}{r}, 2^{\min\{r, m-r\}}]\!]$ QRM code family [38, 41] as a proof of concept. Although implementation of concatenated codes generally assumes all-to-all qubit connectivity [5], a set of systematic construction procedures enlarges the code design space for more future explorations.

It is possible to start from a given CSS code and to seek to identify all logical diagonal gates that can be implemented transversally (see Webster et al. [67, 68]). We take the complementary approach of starting with a target logical diagonal operator and seeking a CSS code that realizes the operator transversally. In this work we provide an algorithmic proof of concept that uses three basic operations. We defer to future work questions about how the number of physical qubits required scales with the level of the target operator in the Clifford hierarchy.

Figure 1 shows how the three basic operations combine to provide CSS codes where both distance and the level of the induced logical operator are increasing. We now examine the three basic operations in more detail.

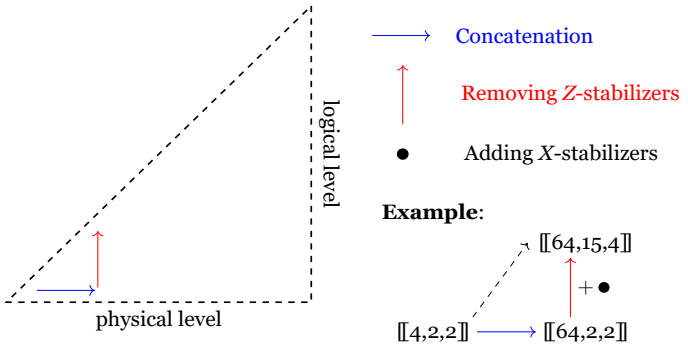

Figure 1 • Three basic operations that can be combined to synthesize a CSS code with higher distance, preserved by a diagonal physical gate that induces a prescribed logical diagonal gate. Graph from [69].

1. **Concatenation**. **Figure 1** shows that the level of the induced logical operator is bounded by that of the physical operator. Concatenation is described in Section 3.1. We double the number of physical qubits to increase the level of the physical diagonal gate and to make room for increasing the level of the induced logical operator. Theorem 1 characterizes the family of physical diagonal gates acting on the new code to induce the same logical gate. For example, the $[\![7, 1, 3]\!]$ Steane code [70] is preserved by a transversal phase gate, $P^{\otimes 7} = \left(Z^{1/2}\right)^{\otimes 7}$, which induces a logical $P^\dagger$ gate. By concatenating once, we obtain the $[\![14, 1, 3]\!]$ CSS code that

supports the logical $P^\dagger$ gate through a family of physical gates including the $I_2^{\otimes 7} \otimes P^{\otimes 7}$ physical gate at level 2 and the transversal T gate ($T^{\otimes 14}$) at level 3. The higher-level gate creates the opportunity to use the second basic operation to increase the level of the induced logical operator. The two operations are as follows:

2. **Removal of Z-stabilizers**. This is described in Section 3.2. We increase the code rate by removing a non-trivial Z-stabilizer to introduce a new logical qubit. Each generator coefficient in the expansion of the original logical operator splits into two new generator coefficients. We provide necessary and sufficient conditions for the new code to be preserved by the original physical diagonal gate. In this case we say that the removal/split is admissible. We describe three types of admissible split that increase the level of the induced logical operator, each built on a recursive relation on the generator coefficients. When the physical gate is a transversal $Z^{1/2^l}$, Theorem 2 specifies the Z-stabilizer that is to be removed. For example, removing the all-one Z-stabilizer from the $[\![14, 1, 3]\!]$ code gives the $[\![14, 2, 2]\!]$ triorthogonal code, and the induced logical operator becomes a transversal $T^\dagger$. Distance may decrease after removing a Z-stabilizer, and the purpose of the third basic operation is to compensate for this loss.

3. **Addition of X-stabilizers**. This is described in Section 3.3. We derive necessary and sufficient conditions for the new code after addition to be preserved by the original physical diagonal gate, and we say that the addition is admissible in this case. Our conditions require that half the generator coefficients associated with the trivial syndrome must vanish. For an admissible addition, we show that the level of the induced logical operator is unchanged. We may need to concatenate several times and to remove several independent Z-stabilizers in order to create sufficiently many zeros to enable an admissible addition. For example, consider the $[\![4, 2, 2]\!]$ CSS code defined by the stabilizer group $\mathcal{S} = \langle X^{\otimes 4}, Z^{\otimes 4}\rangle$. Up to some logical Pauli Z, the code realizes a logical CZ by a transversal phase gate. We first concatenate 4 times to obtain the $[\![64, 2, 2]\!]$ CSS code with the same logical operator, but induced by a physical transversal T gate. Then, we remove 19 independent Z-stabilizers to produce the $[\![64, 21, 2]\!]$ code that realizes 15 logical CCZ gates (up to logical Pauli Z) induced by a physical transversal T gate. Finally, we add 6 independent X-stabilizers to increase the distance and arrive at the $[\![64, 15, 4]\!]$ QRM code supporting the same physical and logical gates.

The next section introduces notation and provides necessary background. Section 3 introduces concatenation, removal of Z-stabilizers, and addition of X-stabilizers, respectively, in its subsections, followed by examples for each basic operation.

2. Background materials, notations and methods

2.1. The pauli group

Any 2×2 Hermitian matrix can be uniquely written as a real linear combination of the four single-qubit Pauli matrices/operators,

$$I_2 := \begin{bmatrix} 1 & 0 \\ 0 & 1 \end{bmatrix}, X := \begin{bmatrix} 0 & 1 \\ 1 & 0 \end{bmatrix}, Z := \begin{bmatrix} 1 & 0 \\ 0 & -1 \end{bmatrix}, \tag{1}$$

and $Y := \imath XZ$, where $\imath := \sqrt{-1}$ is the imaginary unit. Each operator is an involution ($X^2 = Y^2 = Z^2 = I_2$), and pairs of operators anti-commute ($XY = -YX,\ XZ = -ZX,\ YZ = -ZY$).

Let $A \otimes B$ denote the Kronecker product (tensor product) of two matrices A and B. Given binary vectors $\boldsymbol{a} = [a_1, a_2, \ldots, a_n]$ and $\boldsymbol{b} = [b_1, b_2, \ldots, b_n]$ with $a_i, b_j \in \{0, 1\}$ and $n \geq 1$, we define the operators

$$D(\boldsymbol{a}, \boldsymbol{b}) := X^{a_1}Z^{b_1} \otimes \cdots \otimes X^{a_n}Z^{b_n}, \tag{2}$$

$$E(\boldsymbol{a}, \boldsymbol{b}) := \imath^{\boldsymbol{a}\boldsymbol{b}^T \bmod 4} D(\boldsymbol{a}, \boldsymbol{b}). \tag{3}$$

Let $\mathbb{F}_2 = \{0, 1\}$ denote the 1-dimensional binary field and $N = 2^n$ for any given $n \geq 1$. We often abuse notation and write $\boldsymbol{a}, \boldsymbol{b} \in \mathbb{F}_2^n$, though entries of vectors are sometimes interpreted in $\mathbb{Z}_4 = \{0, 1, 2, 3\}$. Note that $D(\boldsymbol{a}, \boldsymbol{b})$ can have order $1, 2$ or 4, but $E(\boldsymbol{a}, \boldsymbol{b})^2 = \imath^{2\boldsymbol{a}\boldsymbol{b}^T} D(\boldsymbol{a}, \boldsymbol{b})^2 = \imath^{2ab^T}(\imath^{2\boldsymbol{a}\boldsymbol{b}^T} I_N) = I_N$. The n-qubit Pauli group is defined as

$$\mathcal{HW}_N := \{\imath^\kappa D(\boldsymbol{a}, \boldsymbol{b}) : \boldsymbol{a}, \boldsymbol{b} \in \mathbb{F}_2^n, \kappa \in \mathbb{Z}_4\}, \tag{4}$$

where $\mathbb{Z}_{2^l} = \{0, 1, \ldots, 2^l - 1\}$. The n-qubit Pauli matrices form an orthonormal basis for the vector space of $N \times N$ complex matrices ($\mathbb{C}^{N\times N}$) under the normalized Hilbert-Schmidt inner product $\langle A, B\rangle := \mathrm{Tr}(A^\dagger B)/N$ [3].

We represent the basis states of a single qubit in $\mathbb{C}^2$ by using the traditional *Dirac notation* $|\cdot\rangle$. For any $\boldsymbol{v} = [v_1, v_2, \cdots, v_n] \in \mathbb{F}_2^n$, we define $|\boldsymbol{v}\rangle = |v_1\rangle \otimes |v_2\rangle \otimes \cdots \otimes |v_n\rangle$, the standard basis vector in $\mathbb{C}^N$ with 1 in the position indexed by $\boldsymbol{v}$ and 0 elsewhere. We write the Hermitian transpose of $|\boldsymbol{v}\rangle$ as $\langle \boldsymbol{v}| = |\boldsymbol{v}\rangle^\dagger$. We may write an arbitrary n-qubit quantum state as $|\psi\rangle = \sum_{\boldsymbol{v}\in\mathbb{F}_2^n} \alpha_{\boldsymbol{v}}|\boldsymbol{v}\rangle \in \mathbb{C}^N$, where $\alpha_{\boldsymbol{v}} \in \mathbb{C}$ and $\sum_{\boldsymbol{v}\in\mathbb{F}_2^n} |\alpha_{\boldsymbol{v}}|^2 = 1$. The Pauli-X operator acts on a single qubit as the bit-flip operator, $X|0\rangle = |1\rangle$ and $X|1\rangle = |0\rangle$, while the Pauli-Z operator flips the phase of the $|1\rangle$ state: $Z|0\rangle = |0\rangle$ and $Z|1\rangle = -|1\rangle$.

The symplectic inner product is $\langle[\boldsymbol{a}, \boldsymbol{b}], [\boldsymbol{c}, \boldsymbol{d}]\rangle_S = \boldsymbol{a}\boldsymbol{d}^T + \boldsymbol{b}\boldsymbol{c}^T \bmod 2$. Since $XZ = -ZX$, we have

$$E(\boldsymbol{a}, \boldsymbol{b})E(\boldsymbol{c}, \boldsymbol{d}) = (-1)^{\langle[\boldsymbol{a},\boldsymbol{b}],[\boldsymbol{c},\boldsymbol{d}]\rangle_S} E(\boldsymbol{c}, \boldsymbol{d})E(\boldsymbol{a}, \boldsymbol{b}). \tag{5}$$

2.2. The Clifford hierarchy

The Clifford hierarchy of unitary operators was introduced in [11]. The first level of the hierarchy is the Pauli group $\mathcal{C}^{(1)} = \mathcal{HW}_N$, which was defined in **(4)**. For $l \geq 2$, the levels l are defined recursively as

$$\mathcal{C}^{(l)} := \{U \in \mathbb{U}_N : U\mathcal{HW}_N U^\dagger \subset \mathcal{C}^{(l-1)}\}, \tag{6}$$

where $\mathbb{U}_N$ is the group of $N \times N$ unitary matrices. The second level is the Clifford Group, $\mathcal{C}^{(2)}$, which can be generated (up

to overall phases) using the "elementary" unitaries *Hadamard*, *Phase*, and either of *Controlled-NOT* (C*X*) or *Controlled-Z* (C*Z*) defined, respectively, as

$$H := \frac{1}{\sqrt{2}}\begin{bmatrix}1 & 1\\ 1 & -1\end{bmatrix}, P := \begin{bmatrix}1 & 0\\ 0 & \imath\end{bmatrix}, \tag{7}$$

$$\mathrm{C}Z_{ab} := |0\rangle\langle 0|_a \otimes (I_2)_b + |1\rangle\langle 1|_a \otimes Z_b, \tag{8}$$

$$\mathrm{C}X_{a\to b} := |0\rangle\langle 0|_a \otimes (I_2)_b + |1\rangle\langle 1|_a \otimes X_b. \tag{9}$$

Note that Clifford unitaries in combination with *any* unitary from a higher level can approximate any unitary operator to any desired precision [10]. In other words, they form a universal set for quantum computation. A widely used choice for the non-Clifford unitary is the *T* gate in the third level defined by

$$T := \begin{bmatrix}1 & 0\\ 0 & e^{\frac{\imath\pi}{4}}\end{bmatrix} = \sqrt{P} = Z^{\frac{1}{4}} \equiv \begin{bmatrix}e^{-\frac{\imath\pi}{8}} & 0\\ 0 & e^{\frac{\imath\pi}{8}}\end{bmatrix} = e^{-\frac{\imath\pi}{8}Z}, \tag{10}$$

where $\equiv$ refers to equal up to a global phase factor, and here the global phase factor is $e^{-\frac{\imath\pi}{8}}$. Note that a global phase factor can be considered as an equivalence because it does not have an observable physical effect.

Let $\mathcal{D}_N$ be the $N \times N$ diagonal matrices, and $\mathcal{C}_d^{(l)} := \mathcal{C}^{(l)} \cap \mathcal{D}_N$. While $\mathcal{C}^{(l)}$ for $l \geq 3$ do not form a group any more, the diagonal gates in each level of the hierarchy, $\mathcal{C}_d^{(l)}$, form a group. Note that $\mathcal{C}_d^{(l)}$ can be generated using the "elementary" unitaries $\mathrm{C}^{(0)}Z^{\frac{1}{2^l}}$, $\mathrm{C}^{(1)}Z^{\frac{1}{2^{l-1}}}, \ldots, \mathrm{C}^{(l-2)}Z^{\frac{1}{2}}$, $\mathrm{C}^{(l-1)}Z$ [12], where $\mathrm{C}^{(i)}Z^{\frac{1}{2^j}} := \sum_{\boldsymbol{u}\in\mathbb{F}_2^{i+1}\setminus\mathbf{1}} |\boldsymbol{u}\rangle\langle\boldsymbol{u}| + e^{\imath\frac{\pi}{2^j}}|\mathbf{1}\rangle\langle\mathbf{1}|$ and here $\mathbf{1} \in \mathbb{F}_2^{i+1}$ is the vector consisting of all ones. In general, the length of $\mathbf{1}$ can change and should be clear in the context. For example, when $i = 1, j = 1$, we have $\mathrm{C}^{(1)}Z^{\frac{1}{2}} = CP = |00\rangle\langle 00| + |01\rangle\langle 01| + |10\rangle\langle 10| + e^{\frac{\imath\pi}{2}}|11\rangle\langle 11|$.

2.3. Stabilizer codes

We define a stabilizer group $\mathcal{S}$ to be a commutative subgroup of the Pauli group $\mathcal{HW}_N$, where every group element is Hermitian and no group element is $-I_N$. We call $\mathcal{S}$ an r-dimensional stabilizer group if it can be generated by r independent elements as $\mathcal{S} = \langle \nu_i E(\boldsymbol{c_i}, \boldsymbol{d_i}) : i = 1, 2, \ldots, r\rangle$, where $\nu_i \in \{\pm 1\}$ and $\boldsymbol{c_i}, \boldsymbol{d_i} \in \mathbb{F}_2^n$. Since $\mathcal{S}$ is commutative, we must have $\langle [\boldsymbol{c_i}, \boldsymbol{d_i}], [\boldsymbol{c_j}, \boldsymbol{d_j}]\rangle_S = \boldsymbol{c_i}\boldsymbol{d_j}^T + \boldsymbol{d_i}\boldsymbol{c_j}^T = 0 \bmod 2$.

The corresponding *stabilizer code* of a a stabilizer group $\mathcal{S}$ is defined as the fixed subspace $\mathcal{V}(\mathcal{S}) := \{|\psi\rangle \in \mathbb{C}^N : g|\psi\rangle = |\psi\rangle \text{ for all } g \in \mathcal{S}\}$. We refer to the subspace $\mathcal{V}(\mathcal{S})$ as an $[[n, k, d]]$ stabilizer code because it encodes $k := n - r$ logical qubits into n physical qubits. The minimum distance d is defined to be the minimum weight of any operator in $\mathcal{N}_{\mathcal{HW}_N}(\mathcal{S}) \setminus \mathcal{S}$. Here, the weight of a Pauli operator is the number of qubits on which it acts non-trivially (i.e., as X, Y or Z), and $\mathcal{N}_{\mathcal{HW}_N}(\mathcal{S})$ denotes the normalizer of $\mathcal{S}$ in $\mathcal{HW}_N$. For example, the weight of $E([1, 1, 0], [1, 0, 0]) = \imath(XZ \otimes X \otimes I)$ is 1 + 1 + 0 = 2, since both $XZ = -\imath Y$ and X act non-trivially.

For any Hermitian Pauli matrix $E(\boldsymbol{c}, \boldsymbol{d})$ and $\nu \in \{\pm 1\}$, the operator $\frac{I_N + \nu E(\boldsymbol{c},\boldsymbol{d})}{2}$ projects onto the ν-eigenspace of $E(\boldsymbol{c}, \boldsymbol{d})$. Thus, the projector onto the codespace $\mathcal{V}(\mathcal{S})$ of the stabilizer code defined by $\mathcal{S} = \langle \nu_i E(\boldsymbol{c_i}, \boldsymbol{d_i}) : i = 1, 2, \ldots, r\rangle$ is

$$\Pi_{\mathcal{S}} = \prod_{i=1}^{r} \frac{(I_N + \nu_i E(\boldsymbol{c_i}, \boldsymbol{d_i}))}{2} = \frac{1}{2^r}\sum_{j=1}^{2^r} \epsilon_j E(\boldsymbol{a_j}, \boldsymbol{b_j}), \tag{11}$$

where $\epsilon_j \in \{\pm 1\}$ is a character of the group $\mathcal{S}$, and is determined by the signs of the generators that produce $E(\boldsymbol{a_j}, \boldsymbol{b_j})$: $\epsilon_j E(\boldsymbol{a_j}, \boldsymbol{b_j}) = \prod_{t\in J\subset\{1,2,\ldots,r\}} \nu_t E(\boldsymbol{c_t}, \boldsymbol{d_t})$ for a unique J.

A *CSS (Calderbank-Shor-Steane) code* is a particular type of stabilizer code with generators that can be separated into strictly X-type and strictly Z-type operators. Consider two classical binary codes $\mathcal{C}_1, \mathcal{C}_2$ such that $\mathcal{C}_2 \subset \mathcal{C}_1$, and let $\mathcal{C}_1^\perp$, $\mathcal{C}_2^\perp$ denote the dual codes. Note that $\mathcal{C}_1^\perp \subset \mathcal{C}_2^\perp$. Suppose that $\mathcal{C}_2 = \langle \boldsymbol{c_1}, \boldsymbol{c_2}, \ldots, \boldsymbol{c_{k_2}}\rangle$ is an $[n, k_2]$ code and $\mathcal{C}_1^\perp = \langle \boldsymbol{d_1}, \boldsymbol{d_2} \ldots, \boldsymbol{d_{n-k_1}}\rangle$ is an $[n, n - k_1]$ code. Then, the corresponding CSS code has the stabilizer group

$$\begin{aligned}\mathcal{S} &= \langle \nu_{(\boldsymbol{c_i},\mathbf{o})} E(\boldsymbol{c_i}, \mathbf{o}), \nu_{(\mathbf{o},\boldsymbol{d_j})} E(\mathbf{o}, \boldsymbol{d_j})\rangle_{i=1;\, j=1}^{i=k_2;\, j=n-k_1}\\ &= \{\epsilon_{(\boldsymbol{a},\mathbf{o})}\epsilon_{(\mathbf{o},\boldsymbol{b})} E(\boldsymbol{a}, \mathbf{o})\, E(\mathbf{o}, \boldsymbol{b}) : \boldsymbol{a} \in \mathcal{C}_2, \boldsymbol{b} \in \mathcal{C}_1^\perp\},\end{aligned}$$

where $\nu_{(\boldsymbol{c_i},\mathbf{o})}, \nu_{(\mathbf{o},\boldsymbol{d_j})}, \epsilon_{(\boldsymbol{a},\mathbf{o})}, \epsilon_{(\mathbf{o},\boldsymbol{b})} \in \{\pm 1\}$. We capture sign information through character vectors $\boldsymbol{y} \in \mathbb{F}_2^n/\mathcal{C}_1, \boldsymbol{r} \in \mathbb{F}_2^n/\mathcal{C}_2^\perp$ such that for any $\epsilon_{(\boldsymbol{a},\mathbf{o})}\epsilon_{(\mathbf{o},\boldsymbol{b})} E(\boldsymbol{a}, \mathbf{o})\, E(\mathbf{o}, \boldsymbol{b}) \in S$, we have $\epsilon_{(\boldsymbol{a},\mathbf{o})} = (-1)^{\boldsymbol{a}\boldsymbol{r}^T}$ and $\epsilon_{(\mathbf{o},\boldsymbol{b})} = (-1)^{\boldsymbol{b}\boldsymbol{y}^T}$. If $\mathcal{C}_1$ and $\mathcal{C}_2^\perp$ can correct up to t errors, then S defines an $[[n, k_1 - k_2, d]]$ CSS code with $d \geq 2t + 1$, which we will represent as $\mathrm{CSS}(X, \mathcal{C}_2, \boldsymbol{r}; Z, \mathcal{C}_1^\perp, \boldsymbol{y})$. If G_2 and $G_1^\perp$ are the generator matrices for $\mathcal{C}_2$ and $\mathcal{C}_1^\perp$ respectively, then the $(n - k_1 + k_2) \times (2n)$ matrix

$$G_{\mathcal{S}} = \left[\begin{array}{c|c} G_2 & \\ \hline & G_1^\perp \end{array}\right] \tag{12}$$

generates $\mathcal{S}$.

Since we consider diagonal gates, the signs of X-stabilizers do not matter. We then assume $\boldsymbol{r} = \mathbf{o}$ in the rest of this paper.

2.4. Generator coefficient framework

The generator coefficient framework was introduced in [38, 39] to describe the evolution of stabilizer code states under a physical diagonal gate $U_Z = \sum_{\boldsymbol{u}\in\mathbb{F}_2^n} d_{\boldsymbol{u}}|\boldsymbol{u}\rangle\langle\boldsymbol{u}|$. Note that $|\boldsymbol{u}\rangle\langle\boldsymbol{u}| = \frac{1}{2^n}\sum_{\boldsymbol{v}\in\mathbb{F}_2^n}(-1)^{\boldsymbol{u}\boldsymbol{v}^T} E(\mathbf{o}, \boldsymbol{v})$. Then we may expand U_Z in the Pauli basis

$$U_Z = \sum_{\boldsymbol{v}\in\mathbb{F}_2^n} f(\boldsymbol{v}) E(\mathbf{o}, \boldsymbol{v}), \tag{13}$$

where

$$f(\boldsymbol{v}) = \frac{1}{2^n}\sum_{\boldsymbol{u}\in\mathbb{F}_2^n}(-1)^{\boldsymbol{u}\boldsymbol{v}^T} d_{\boldsymbol{u}}. \tag{14}$$

Note that we can connect the coefficients in standard basis and Pauli basis as

$$[f(\boldsymbol{v})]_{\boldsymbol{v}\in\mathbb{F}_2^n} = [d_{\boldsymbol{u}}]_{\boldsymbol{u}\in\mathbb{F}_2^n} H_{2^n}, \tag{15}$$

where $H_{2^n} = H \otimes H_{2^{n-1}} = H^{\otimes n}$ is the Walsh-Hadamard matrix.

We consider the average logical channel induced by U_Z of an $[\![n, k, d]\!]$ $\mathrm{CSS}(X, \mathcal{C}_2; Z, \mathcal{C}_1^\perp, \boldsymbol{y})$ code as described in **Figure 2**. Let $B_{\boldsymbol{\mu}}$ be the induced logical operator corresponding to the syndrome $\boldsymbol{\mu}$. Then the evolution of code states can be described as

$$\rho_4 = \sum_{\boldsymbol{\mu}\in\mathbb{F}_2^n/\mathcal{C}_2^\perp} B_{\boldsymbol{\mu}}\rho_1 B_{\boldsymbol{\mu}}^\dagger. \tag{16}$$

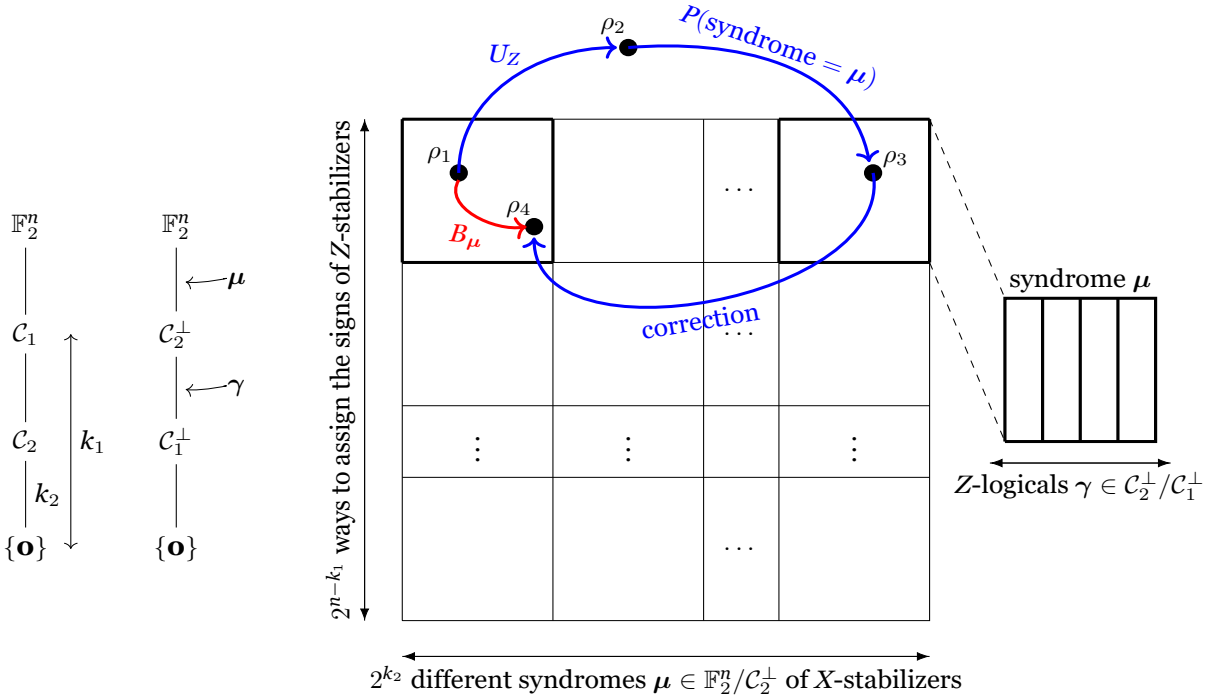

Figure 2 • The 2^{n-k_1} rows of the array are indexed by the $[\![n, k_1 - k_2, d]\!]$ CSS codes corresponding to all possible signs of the Z-stabilizer group. The 2^{k_2} columns of the array are indexed by all possible X-syndromes $\boldsymbol{\mu}$. The logical operator B_μ is induced by (1) preparing any code state ρ_1; (2) applying a diagonal physical gate U_Z to obtain ρ_2; (3) using X-stabilizers to measure ρ_2, obtaining the syndrome $\boldsymbol{\mu}$ with probability p_μ, and the post-measurement state ρ_3; (4) applying a Pauli correction to ρ_3, obtaining ρ_4. Graph from [38].

The generator coefficients $A_{\mu,\gamma}$ are obtained by expanding the logical operator B_μ in terms of Z-logical Pauli operators $\epsilon_{(\mathbf{o},\gamma)}E(\mathbf{o},\gamma)$,

$$B_\mu = \epsilon_{(\mathbf{o},\gamma_\mu)}E(\mathbf{o},\gamma_\mu)\sum_{\gamma\in\mathcal{C}_2^\perp/\mathcal{C}_1^\perp} A_{\mu,\gamma}\,\epsilon_{(\mathbf{o},\gamma)}E(\mathbf{o},\gamma), \tag{17}$$

where $\epsilon_{(\mathbf{o},\gamma_\mu)}E(\mathbf{o},\gamma_\mu)$ models the Z-logical Pauli operator introduced by a decoder. For each pair of a X-syndrome $\boldsymbol{\mu} \in \mathbb{F}_2^n/\mathcal{C}_2^\perp$ and a Z-logical $\boldsymbol{\gamma} \in \mathcal{C}_2^\perp/\mathcal{C}_1^\perp$, the generator coefficient $A_{\mu,\gamma}$ corresponding to U_Z is

$$A_{\mu,\gamma} \coloneqq \sum_{\boldsymbol{z}\in\mathcal{C}_1^\perp+\boldsymbol{\mu}+\boldsymbol{\gamma}} \epsilon_{(\mathbf{o},\boldsymbol{z})}f(\boldsymbol{z}), \tag{18}$$

where $\epsilon_{(\mathbf{o},\boldsymbol{z})} = (-1)^{\boldsymbol{z}\boldsymbol{y}^T}$ is the sign of the Z-stabilizer $E(\mathbf{o},\boldsymbol{z})$. Based on the structure of CSS codes, generator coefficients group the Pauli coefficients of U_Z together, and tune them by the signs of Z-stabilizer. We use **(14)** to simplify **(18)** as

$$\begin{aligned} A_{\mu,\gamma} &= \frac{1}{2^n}\sum_{\boldsymbol{u}\in\mathbb{F}_2^n}\sum_{\boldsymbol{z}\in\mathcal{C}_1^\perp+\boldsymbol{\mu}+\boldsymbol{\gamma}} (-1)^{\boldsymbol{z}\boldsymbol{y}^T}(-1)^{\boldsymbol{z}\boldsymbol{u}^T}d_{\boldsymbol{u}} \\ &= \frac{1}{|\mathcal{C}_1|}\sum_{\boldsymbol{u}\in\mathcal{C}_1+\boldsymbol{y}} (-1)^{(\boldsymbol{\mu}\oplus\boldsymbol{\gamma})(\boldsymbol{y}\oplus\boldsymbol{u})^T}d_{\boldsymbol{u}}. \end{aligned} \tag{19}$$

The diagonal physical gate U_Z preserves a CSS$(X,\mathcal{C}_2;Z,\mathcal{C}_1^\perp,\boldsymbol{y})$ codespace if and only if $B_{\mu=\mathbf{o}}$ is a unitary [38], which is equivalent to requiring

$$\sum_{\gamma\in\mathcal{C}_2^\perp/\mathcal{C}_1^\perp} |A_{\mathbf{o},\gamma}|^2 = 1. \tag{20}$$

Note that **(20)** is also equivalent to $A_{\mu\neq\mathbf{o},\gamma} = 0$ for all $\boldsymbol{\gamma} \in \mathcal{C}_2^\perp/\mathcal{C}_1^\perp$. The induced logical operator is

$$U_Z^L = \sum_{\boldsymbol{\alpha}\in\mathbb{F}_2^k} A_{\mathbf{o},g(\boldsymbol{\alpha})}E(\mathbf{o},\boldsymbol{\alpha}), \tag{21}$$

where $g : \mathbb{F}_2^k \to \mathcal{C}_2^\perp/\mathcal{C}_1^\perp$ is a bijective map defined by $g(\boldsymbol{\alpha}) = \boldsymbol{\alpha}G_{\mathcal{C}_2^\perp/\mathcal{C}_1^\perp}$, and $G_{\mathcal{C}_2^\perp/\mathcal{C}_1^\perp}$ is a generator matrix of the Z-logicals $\mathcal{C}_2^\perp/\mathcal{C}_1^\perp$.

3. Results

3.1. Climbing the physical hierarchy

We need to climb the physical Clifford hierarchy because the level of the physical operator bounds that of the induced logical operator. Consider a physical diagonal gate

$$U_Z = \sum_{\boldsymbol{u}\in\mathbb{F}_2^n} d_{\boldsymbol{u}}|\boldsymbol{u}\rangle\langle\boldsymbol{u}|, \tag{22}$$

that preserves an $[\![n,k,d]\!]$ CSS$(X,\mathcal{C}_2;Z,\mathcal{C}_1^\perp,\boldsymbol{y})$ code with X-distance

$$d_X \coloneqq \min_{\boldsymbol{x}\in\mathcal{C}_1\setminus\mathcal{C}_2} w_H(\boldsymbol{x}), \tag{23}$$

and Z-distance

$$d_Z \coloneqq \min_{\boldsymbol{z}\in\mathcal{C}_2^\perp\setminus\mathcal{C}_1^\perp} w_H(\boldsymbol{z}). \tag{24}$$

We denote the logical operator induced by U_Z as U_Z^L. The concatenation process described in **Figure 3** produces a $[\![2n,k,d']\!]$ CSS$(X,\mathcal{C}_2';Z,(\mathcal{C}_1')^\perp,\boldsymbol{y}')$ code. Concatenation does not change the number of Z-logicals or the number of X-syndromes, and so the number of generator coefficients remains the same. We now show this code is preserved by an ensemble of physical gates, all inducing the same logical operator as U_Z^L.

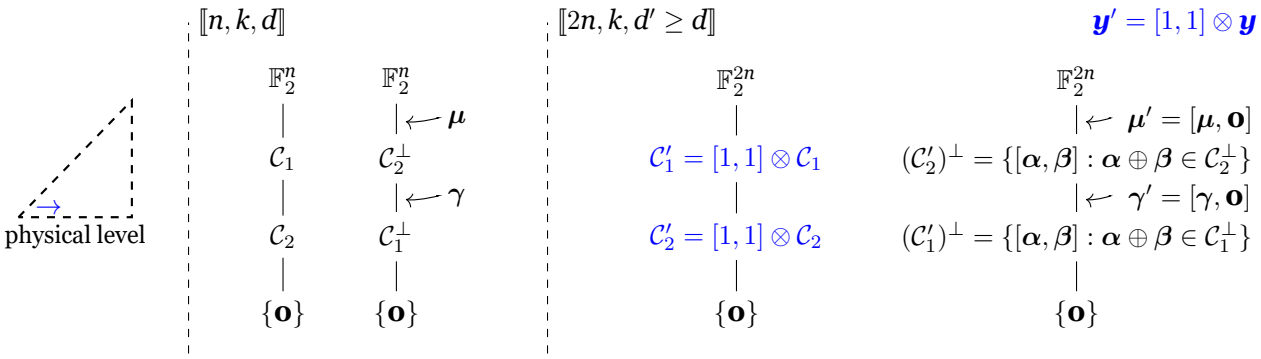

Figure 3 • Concatenation transforms an $[\![n,k,d]\!]$ CSS code preserved by a diagonal gate U_Z at level l to a $[\![2n,k,d']\!]$ CSS code preserved by a family of diagonal gates U_Z', some of which are at level $l+1$ such as $\left(\sqrt{U_Z}\right)^{\otimes 2}$. The logical operator induced by U_Z' coincides with the logical operator induced by U_Z. Graph from [69].

Theorem 1. *The $[\![2n,k,d']\!]$ CSS$(X,\mathcal{C}_2';Z,(\mathcal{C}_1')^\perp,\boldsymbol{y}')$ code is preserved by any diagonal physical gate*

$$U_Z'=\sum_{\boldsymbol{u}'\in\mathbb{F}_2^{2n}} d'_{\boldsymbol{u}'}|\boldsymbol{u}'\rangle\langle\boldsymbol{u}'|, \tag{25}$$

for which $d'_{[\boldsymbol{u},\boldsymbol{u}]}=d_{\boldsymbol{u}}$ for all $\boldsymbol{u}\in\mathbb{F}_2^n$.

The minimum distance $d'\geq d$ and the induced logical operator $(U_Z')^L$ is equal to U_Z^L.

Proof. Let d_X',d_Z' be the X- and Z-distances for the CSS$(X,\mathcal{C}_2';Z,(\mathcal{C}_1')^\perp,\boldsymbol{y}')$ code. Given $\boldsymbol{x}'\in\mathcal{C}_1'\setminus\mathcal{C}_2'$, there exists $\boldsymbol{x}\in\mathcal{C}_1\setminus\mathcal{C}_2$ such that $\boldsymbol{x}'=[1,1]\otimes\boldsymbol{x}$, and so $d_X'=2d_X$. Given $[\boldsymbol{\alpha},\boldsymbol{\beta}]\in(\mathcal{C}_2')^\perp\setminus(\mathcal{C}_1')^\perp$, we have

$$w_H([\boldsymbol{\alpha},\boldsymbol{\beta}])=w_H(\boldsymbol{\alpha})+w_H(\boldsymbol{\beta})\geq w_H(\boldsymbol{\alpha}\oplus\boldsymbol{\beta}), \tag{26}$$

and so $d_Z'\geq d_Z$. Concatenation doubles X-distance while maintaining Z-distance.

We now prove that $(U_Z')^L=U_Z^L$ by showing the generator coefficients remain the same:

$$\begin{aligned}
A'_{\boldsymbol{\mu}',\boldsymbol{\gamma}'}(U_Z') &= \frac{1}{|\mathcal{C}_1'|}\sum_{\boldsymbol{u}'\in\mathcal{C}_1'+\boldsymbol{y}'}(-1)^{(\boldsymbol{\mu}'\oplus\boldsymbol{\gamma}')(\boldsymbol{y}'\oplus\boldsymbol{u}')^T}d'_{\boldsymbol{u}'}\\
&= \frac{1}{|\mathcal{C}_1|}\sum_{\boldsymbol{u}\in\mathcal{C}_1+\boldsymbol{y}}(-1)^{[\boldsymbol{\mu}\oplus\boldsymbol{\gamma},\mathbf{0}][\boldsymbol{y}\oplus\boldsymbol{u},\boldsymbol{y}\oplus\boldsymbol{u}]^T}d'_{[\boldsymbol{u},\boldsymbol{u}]}\\
&= \frac{1}{|\mathcal{C}_1|}\sum_{\boldsymbol{u}\in\mathcal{C}_1+\boldsymbol{y}}(-1)^{(\boldsymbol{\mu}\oplus\boldsymbol{\gamma})(\boldsymbol{y}\oplus\boldsymbol{u})^T}d_{\boldsymbol{u}}\\
&= A_{\boldsymbol{\mu},\boldsymbol{\gamma}}(U_Z).
\end{aligned} \tag{27}$$

Hence, concatenation brings more freedom of physical operators to realize the same logical operator. □

We may partition U_Z' into 2^n blocks, where the block indexed by $\boldsymbol{u}\in\mathbb{F}_2^n$ is a $2^n\times 2^n$ diagonal matrix $\mathrm{diag}[d'_{[\boldsymbol{u},\boldsymbol{v}]}]$. Theorem 1 specifies a single diagonal entry $d'_{[\boldsymbol{u},\boldsymbol{u}]}$ in each block. The remaining $2^{2n}-2^n$ entries can be freely chosen to design the unitary U_Z'. When U_Z (on n qubits) is a transversal $\mathrm{C}^{(i)}Z^{1/2^j}$ gate at level $i+j$ in the clifford hierarchy, we can choose U_Z' to be the transversal $\mathrm{C}^{(i)}Z^{1/2^{j+1}}$ gate (on $2n$ qubits) at level $i+j+1$.

Remark 1. (Quadratic Form Diagonal (QFD) gates). *We now describe how to raise the level of a QFD gate $\tau_R^{(l)}\in\mathcal{C}_d^{(l)}$ at level l in the Clifford hierarchy. Here*

$$\tau_R^{(l)}=\sum_{\boldsymbol{v}\in\mathbb{F}_2^n}\xi_l^{\boldsymbol{v}R\boldsymbol{v}^T \bmod 2^l}|\boldsymbol{v}\rangle\langle\boldsymbol{v}|, \tag{28}$$

where $\xi_l=e^{\imath\frac{\pi}{2^{l-1}}}$, and R is an $n\times n$ symmetric matrix with entries in $\mathbb{Z}_{2^l}$, the ring of integers modulo 2^l. Note that the exponent $\boldsymbol{v}R\boldsymbol{v}^T\in\mathbb{Z}_{2^l}$. Rengaswamy et al. [16] proved that QFD gates include all 1-local and 2-local diagonal gates in the Clifford hierarchy. We choose $U_Z'=\tau_{I_2\otimes R}^{(l+1)}\in\mathcal{C}_d^{(l+1)}$, and observe

$$d'_{\boldsymbol{u},\boldsymbol{u}}=\xi_{l+1}^{2\boldsymbol{u}R\boldsymbol{u}^T}=\xi_l^{\boldsymbol{u}R\boldsymbol{u}^T}=d_{\boldsymbol{u}}. \tag{29}$$

Example 1. (Climbing from $P^{\otimes 7}$ acting on the $[\![7,1,3]\!]$ Steane code to $T^{\otimes 14}$ acting on the $[\![14,1,3]\!]$ CSS code). *The Steane code [70] is a CSS$(X,\mathcal{C}_2;Z,\mathcal{C}_1^\perp,\boldsymbol{y}=\mathbf{0})$ code with generator matrix*

$$G_{\mathcal{S}}=\left[\begin{array}{c|c} H & \\ \hline & H\end{array}\right], \tag{30}$$

where H is the parity-check matrix of the Hamming code:

$$H=\begin{bmatrix}1&1&1&1&0&0&0\\1&1&0&0&1&1&0\\1&0&1&0&1&0&1\end{bmatrix}. \tag{31}$$

*The only nontrivial Z-logical corresponds to the all one vector $\mathbf{1}$. After concatenation described in **Figure 3**, we obtain a $[\![14,1,3]\!]$ CSS code. When $R=I_n$, $\tau_R^{(2)}=P^{\otimes n}$ and $\tau_{I_2\otimes R}^{(3)}=T^{\otimes 2n}$. Let $A_{\mu,\gamma}\left(\frac{\pi}{2}\right)$ and $A'_{\mu',\gamma'}\left(\frac{\pi}{4}\right)$ be the generator coefficients corresponding to $P^{\otimes 7}$ and $T^{\otimes 14}$ acts on the $[\![7,1,3]\!]$ and $[\![14,1,3]\!]$ code respectively. Then, we have*

$$\begin{aligned}
A_{\mu=\mathbf{0},\gamma=\mathbf{0}}\left(\frac{\pi}{2}\right)&=A'_{[\mathbf{0},\mathbf{0}],[\mathbf{1},\mathbf{0}]}\left(\frac{\pi}{4}\right)=\cos\left(\frac{\pi}{4}\right),\\
A_{\mu=\mathbf{0},\gamma=\mathbf{1}}\left(\frac{\pi}{2}\right)&=A'_{[\mathbf{0},\mathbf{0}],[\mathbf{1},\mathbf{0}]}\left(\frac{\pi}{4}\right)=\imath\sin\left(\frac{\pi}{4}\right),
\end{aligned} \tag{32}$$

*which implies that the invariance of $[\![7,1,3]\!]$ under $P^{\otimes 7}$ and that of $[\![14,1,3]\!]$ under $T^{\otimes 14}$. It then follows from the expression of the induced logical operator in **(21)** that both of the codes implement a logical $P^\dagger$.*

Example 2. Climbing from $\mathrm{C}Z^{\otimes 2}$ acting on the $[\![4,2,2]\!]$ CSS code to $\mathrm{C}P^{\otimes 4}$ acting on the $[\![8,2,2]\!]$ CSS code). *Consider the $[\![4,2,2]\!]$ CSS$(X,\mathcal{C}_2;Z,\mathcal{C}_1^\perp)$ code with $\mathcal{C}_2=\mathcal{C}_1^\perp=\{\mathbf{0},\mathbf{1}\}$. We may choose the*

generators of Z-logicals to be $\boldsymbol{\gamma_1} = [0,0,1,1]$ *and* $\boldsymbol{\gamma_2} = [0,1,1,0]$. *Their generator coefficients coincide:*

$$\begin{aligned} A_{\boldsymbol{\mu}=\mathbf{o},\boldsymbol{\gamma}=\mathbf{o}}(\mathrm{CZ}^{\otimes 2}) &= A'_{[\mathbf{o},\mathbf{o}],[\mathbf{o},\mathbf{o}]}(\mathrm{CP}^{\otimes 4}) = \frac{1}{2}, \\ A_{\boldsymbol{\mu}=\mathbf{o},\boldsymbol{\gamma}=\boldsymbol{\gamma_1}}(\mathrm{CZ}^{\otimes 2}) &= A'_{[\mathbf{o},\mathbf{o}],[\boldsymbol{\gamma_1},\mathbf{o}]}(\mathrm{CP}^{\otimes 4}) = -\frac{1}{2}, \\ A_{\boldsymbol{\mu}=\mathbf{o},\boldsymbol{\gamma}=\boldsymbol{\gamma_2}}(\mathrm{CZ}^{\otimes 2}) &= A'_{[\mathbf{o},\mathbf{o}],[\boldsymbol{\gamma_2},\mathbf{o}]}(\mathrm{CP}^{\otimes 4}) = \frac{1}{2}, \\ A_{\boldsymbol{\mu}=\mathbf{o},\boldsymbol{\gamma}=\boldsymbol{\gamma_1}\oplus\boldsymbol{\gamma_2}}(\mathrm{CZ}^{\otimes 2}) &= A'_{[\mathbf{o},\mathbf{o}],[\boldsymbol{\gamma_1}\oplus\boldsymbol{\gamma_2},\mathbf{o}]}(\mathrm{CP}^{\otimes 4}) = \frac{1}{2}. \end{aligned} \tag{33}$$

Both cases realize a logical $Z_1 \circ CZ \coloneqq (Z \otimes I)\mathrm{CZ}$.

Remark 2. (Switching between Computation and Storage). *It is the choice of character vector that distinguishes the method of concatenation depicted in* ***Figure 3*** *from the method of constructing a decoherence-free subspace (DFS) described in [52]. Consider the graph where the vertices are the qubits involved in the support of some X-stabilizer, and where two vertices are joined by an edge if there exists a weight 2 Z-stabilizer involving these two qubits. Instead of choosing* $\boldsymbol{y}' = [1,1] \otimes \boldsymbol{y}$, *Liang, Hu et al. [52] balance the signs of Z-stabilizers by requiring that the support of* $\boldsymbol{y}''$ *include half the qubits in every connected component of the graph. The stabilizer group determines a resolution of the identity. To change the signs of Z-stabilizers, we simply apply some physical Pauli X to transform from one part of the resolution to the other part (see [38] (Example 3) for more details). To determine the specific position to add these extra Pauli X, we consider the general encoding map* $g_e : |\boldsymbol{\alpha}\rangle_L \in \mathbb{F}_2^k \to |\overline{\boldsymbol{\alpha}}\rangle \in \mathcal{V}(\mathcal{S})$ *of a CSS*$(X, \mathcal{C}_2, \boldsymbol{r}; Z, \mathcal{C}_1^\perp, \boldsymbol{y})$ *code [38],*

$$|\overline{\boldsymbol{\alpha}}\rangle \coloneqq \frac{1}{\sqrt{|\mathcal{C}_2|}} \sum_{\boldsymbol{x}\in\mathcal{C}_2} (-1)^{\boldsymbol{x}\boldsymbol{r}^T} |\boldsymbol{\alpha} G_{\mathcal{C}_1/\mathcal{C}_2} \oplus \boldsymbol{x} \oplus \boldsymbol{y}\rangle, \tag{34}$$

where $\boldsymbol{r}, \boldsymbol{y}$ *are the character vectors for X- and Z-stabilizers, and* $G_{\mathcal{C}_1/\mathcal{C}_2}$ *is a generator matrix of the X-logicals* $\mathcal{C}_1/\mathcal{C}_2$. *The positions of these Pauli X correspond to the support of the difference of two character vectors* $\boldsymbol{y}' - \boldsymbol{y}''$. *Hence, it is simple to switch between computation and storage. Given a code that realizes a specific diagonal logical operator induced by the physical gate* U_Z, *we first apply the concatenation described in* ***Figure 3***. *After concatenation, we choose* $U'_Z = I_N \otimes U_Z$, *at the same level as* U_Z, *to realize the same specific logical operator. We then apply some physical Pauli X to change signs of Z-stabilizers and embed the logical information in a DFS. To continue the computation, we recover the stored results by applying the same Pauli X. Note that concatenation doubles the X-distance, which improves protection when we change the signs of Z-stabilizers.*

For example, suppose our goal is to first implement a logical $P^\dagger$ *and to wait for a while before calculating the next step. We can apply the physical* $U'_Z = I_2^{\otimes 7} \otimes P^{\otimes 7}$ *to the* $[\![14,1,3]\!]$ *CSS code in Example 1 to realize the logical* $P^\dagger$. *Note that* $\boldsymbol{y}' = \mathbf{o} \in \mathbb{F}_2^{14}$ *and one choice of* $\boldsymbol{y}''$ *is* $[1,0] \otimes \mathbf{1}_7 \in \mathbb{F}_2^{14}$. *Then we can apply Pauli X alternatively to map the computed result in a DFS (See [71] for more details).*

To achieve more advanced computation, we need diagonal logical operators from higher levels. Raising the level of a physical operator prepares the ground for climbing the logical hierarchy.

3.2. Climbing the logical hierarchy

In this section, we describe how to increase the level of an induced logical operator by judiciously removing Z-stabilizers from a CSS code. We start by considering a physical diagonal gate

$$U_Z = \sum_{\boldsymbol{v}\in\mathbb{F}_2^n} f(\boldsymbol{v}) E(\mathbf{o}, \boldsymbol{v}) \tag{35}$$

that preserves an $[\![n,k,d]\!]$ CSS$(X, \mathcal{C}_2; Z, \mathcal{C}_1^\perp, \boldsymbol{y})$ code. The induced logical channels are described by generator coefficients $A_{\boldsymbol{\mu},\boldsymbol{\gamma}}$ where $\boldsymbol{\mu} \in \mathbb{F}_2^n/\mathcal{C}_2^\perp$ and $\boldsymbol{\gamma} \in \mathcal{C}_2^\perp/\mathcal{C}_1^\perp$. Let $\boldsymbol{\gamma_0} \in \mathcal{C}_1^\perp$ be a nontrivial Z-stabilizer. Set $\mathcal{C}_1^\perp = \langle (\mathcal{C}'_1)^\perp, \boldsymbol{\gamma_0}\rangle$, and set $\mathcal{C}'_1 = \langle \mathcal{C}_1, \boldsymbol{w_o}\rangle$, where $\boldsymbol{w_o} \in \mathbb{F}_2^n/\mathcal{C}_1$. If we remove $\boldsymbol{\gamma_0}$ from $\mathcal{C}_1^\perp$, then $\boldsymbol{\gamma_0}$ becomes a Z-logical for the $[\![n, k+1, d' \le d]\!]$ CSS$(X, \mathcal{C}_2; Z, (\mathcal{C}'_1)^\perp, \boldsymbol{y})$ code, as shown in **Figure 4a**. Removing the Z-logical $\boldsymbol{\gamma_0}$ doubles the number of Z-logicals. Each generator coefficient $A_{\boldsymbol{\mu},\boldsymbol{\gamma}}$ associated with the original CSS code splits into two generator coefficients $A'_{\boldsymbol{\mu},\boldsymbol{\gamma}'=\boldsymbol{\gamma}}$ and $A'_{\boldsymbol{\mu},\boldsymbol{\gamma}'=\boldsymbol{\gamma}\oplus\boldsymbol{\gamma_0}}$ associated with the new code. We have

$$\begin{aligned} A_{\boldsymbol{\mu},\boldsymbol{\gamma}} &= \sum_{\boldsymbol{z}\in\langle(\mathcal{C}'_1)^\perp,\boldsymbol{\gamma_0}\rangle+\boldsymbol{\mu}+\boldsymbol{\gamma}} \epsilon_{(\mathbf{o},\boldsymbol{z})} f(\boldsymbol{z}) \\ &= \sum_{\boldsymbol{z}\in(\mathcal{C}'_1)^\perp+\boldsymbol{\mu}+\boldsymbol{\gamma}} \epsilon_{(\mathbf{o},\boldsymbol{z})} f(\boldsymbol{z}) \\ &\quad + \sum_{\boldsymbol{z}\in(\mathcal{C}'_1)^\perp+\boldsymbol{\mu}+\boldsymbol{\gamma}+\boldsymbol{\gamma_0}} \epsilon_{(\mathbf{o},\boldsymbol{z})} f(\boldsymbol{z}) \\ &= A'_{\boldsymbol{\mu},\boldsymbol{\gamma}'=\boldsymbol{\gamma}} + A'_{\boldsymbol{\mu},\boldsymbol{\gamma}'=\boldsymbol{\gamma}\oplus\boldsymbol{\gamma_0}}. \end{aligned} \tag{36}$$

Adding a Z-stabilizer simply reverses this process as shown in **Figure 4b**.

Definition 1. (Admissible Splits). *A split is admissible if the physical diagonal gate* U_Z *preserves the CSS*$(X, \mathcal{C}_2; Z, (\mathcal{C}'_1)^\perp, \boldsymbol{y})$ *code obtained by removing the non-trivial Z-stabilizer* $\boldsymbol{\gamma_0}$.

Since U_Z preserves the original CSS code, we have

$$\sum_{\boldsymbol{\gamma}\in\mathcal{C}_2^\perp/\mathcal{C}_1^\perp} |A_{\mathbf{o},\boldsymbol{\gamma}}|^2 = 1. \tag{37}$$

The condition

$$\begin{aligned} \sum_{\boldsymbol{\gamma}'\in\langle\mathcal{C}_2^\perp/\mathcal{C}_1^\perp,\boldsymbol{\gamma_0}\rangle} |A'_{\mathbf{o},\boldsymbol{\gamma}'}|^2 &= \sum_{\boldsymbol{\gamma}\in\mathcal{C}_2^\perp/\mathcal{C}_1^\perp} |A'_{\mathbf{o},\boldsymbol{\gamma}}|^2 + |A'_{\mathbf{o},\boldsymbol{\gamma}\oplus\boldsymbol{\gamma_0}}|^2 \\ &= 1 \end{aligned} \tag{38}$$

is both necessary and sufficient for admissibility. Note that the induced logical operator **(21)** corresponding to the trivial syndrome remains a diagonal unitary after splitting.

It is natural to ask how many Z-stabilizers are needed to determine a stabilizer code fixed by a given family of diagonal physical operators U_Z. Liang, Hu et al. [52] derived necessary and sufficient conditions for all transversal Z-rotations to preserve the codespace of a stabilizer code. The conditions require the weight 2 Z-stabilizers to cover all the qubits that are in the support of the X-component of some stabilizer. Rengaswamy et al. [41] derived less restrictive necessary and sufficient conditions for a single transversal T gate.

The difference $A'_{\mathbf{o},\boldsymbol{\gamma}} - A'_{\mathbf{o},\boldsymbol{\gamma}\oplus\boldsymbol{\gamma_0}}$ depends on the new X-logical $\boldsymbol{w_o}$. For $\boldsymbol{\gamma} \in \mathcal{C}_2^\perp/\mathcal{C}_1^\perp$, let

$$s_{\boldsymbol{\gamma}}(\boldsymbol{w_o}) \coloneqq \frac{1}{|\mathcal{C}_1|} \sum_{\boldsymbol{u}\in\mathcal{C}_1+\boldsymbol{w_o}} (-1)^{\boldsymbol{\gamma}\boldsymbol{u}^T} d_{\boldsymbol{u}\oplus\boldsymbol{y}}. \tag{39}$$

It then follows from **(19)** that

$$A'_{\mathbf{o},\gamma} = \frac{1}{2|\mathcal{C}_1|} \sum_{\boldsymbol{u}\in\langle \mathcal{C}_1, \boldsymbol{w_o}\rangle} (-1)^{\boldsymbol{\gamma u}^T} d_{\boldsymbol{u}\oplus\boldsymbol{y}}$$
$$= \frac{1}{2}\left(A_{\mathbf{o},\gamma} + s_\gamma(\boldsymbol{w_o})\right), \tag{40}$$

and follows from **(36)** that

$$A'_{\mathbf{o},\gamma\oplus\gamma_0} = \frac{1}{2}\left(A_{\mathbf{o},\gamma} - s_\gamma(\boldsymbol{w_o})\right). \tag{41}$$

The quantity $s_\gamma(\boldsymbol{w_o})$ determines whether or not a split is admissible.

We design extensible splittings by expanding diagonal operators in the Pauli basis, and we illustrate our approach by constructing $Z^{1/2^l}\otimes Z^{1/2^l}$ from $Z^{1/2^{l-1}}$. We write

$$Z^{1/2^{l-1}} \equiv c_l I + s_l Z, \tag{42}$$

where $c_l := \cos\pi/2^l$, $s_l := -\imath\sin\pi/2^l$, and where $\equiv$ denotes equality to within a global phase factor $e^{-\imath\pi/2^l}$. Note that the scalar multiplying a tensor product is simply the product of scalars multiplying individual components, and that measurement probabilities are independent of any global phase factor. **Figure 5a** shows how we construct

$$\left(Z^{1/2^l}\right)^{\otimes 2} \equiv c_{l+1}^2 I\otimes I + c_{l+1}s_{l+1}(I\otimes Z + Z\otimes I)$$
$$+ s_{l+1}^2 Z\otimes Z, \tag{43}$$

by making use of the double-angle formulas

$$c_l = c_{l+1}^2 + s_{l+1}^2 \text{ and } s_l = 2c_{l+1}s_{l+1}. \tag{44}$$

For example, the logical gate P can be connected to $T^{\otimes}2$ at a higher level in the Clifford hierarchy. Recall that generator coefficients coincide with Pauli coefficients of the induced logical operator as described in **(21)**. The splitting rule determines the values $s_\gamma(\boldsymbol{w_o})$ needed to satisfy **(40)** and **(41)**. Here we require

$$s_\gamma(\boldsymbol{w_o}) = \begin{cases} 1, & \text{if } \boldsymbol{\gamma} = \mathbf{o}, \\ 0, & \text{if } \boldsymbol{\gamma} \neq \mathbf{o}, \end{cases} \tag{45}$$

since we can write double-angle formulas as

$$c_{l+1}^2 = \frac{1}{2}(c_l + 1),\ s_{l+1}^2 = \frac{1}{2}(c_l - 1), \tag{46}$$
$$\text{and } s_{l+1}c_{l+1} = \frac{1}{2}(s_l + 0). \tag{47}$$

Note that this design only connects a single level in the Clifford hierarchy to the next level, that it does not extend indefinitely. In **Figure 5b**, we generalize the design to make it extend indefinitely. We include the global phase $x_l := e^{\imath\pi/2^l}$ this time, and decompose part of x_l using the Euler's formula

$$x_l = x_{l+1}x_{l+1} = x_{l+1}(c_{l+1} - s_{l+1}). \tag{48}$$

Note that $Z^{1/2^{l-1}} = x_l(c_l I + s_l Z)$ and $\left(Z^{1/2^l}\right)^\dagger = \frac{x_{l+1}}{x_l}(c_{l+1}I - s_{l+1}Z)$. Then after splitting, we obtain the gate in one level higher

$$Z^{1/2^{l-1}}\otimes\left(Z^{1/2^l}\right)^\dagger = x_{l+1}(c_l c_{l+1} I\otimes I - c_l s_{l+1} I\otimes Z$$
$$+ s_l c_{l+1} Z\otimes I - s_l s_{l+1} Z\otimes Z). \tag{49}$$

The decomposition in **(48)** holds for any l, and we can use induction to prove that after splitting j times, we obtain the gate

$$Z^{1/2^{l-1}}\otimes\left(Z^{1/2^l}\right)^\dagger\otimes\cdots\otimes\left(Z^{1/2^{l-1+j}}\right)^\dagger. \tag{50}$$

Because of the non-uniform rotations, the values $s_\gamma(\boldsymbol{w_o})$ needed to satisfy vary from step to step. We now introduce a splitting that is indefinitely extensible with simple requirement for $s_\gamma(\boldsymbol{w_o})$.

The diagonal operator $\mathrm{C}^{(j-1)}Z^{1/2^{l-1}} = \mathrm{diag}[\boldsymbol{d_j}]$ for

$$\boldsymbol{d_j} = [\mathbf{1}_{2^{j-1}}, \mathbf{1}_{2^{j-1}-1}, x_{l-1}]^T, \tag{51}$$

where $\mathbf{1}_m$ is the all-one vector with length m. Let $\boldsymbol{e_1},\ldots,\boldsymbol{e_{2^j}}$ be the standard basis of $\mathbb{F}_2^{2^j}$.We expand $\mathrm{C}^{(j-1)}Z^{1/2^{l-1}}$ in the Pauli basis using the Walsh-Hadamard matrix H_{2^j},

$$\mathrm{C}^{(j-1)}Z^{1/2^{l-1}} = \sum_{\boldsymbol{v}\in\mathbb{F}_2^j} c_j(\boldsymbol{v})E(\mathbf{o},\boldsymbol{v}), \tag{52}$$

where $\boldsymbol{c_j} := [c_j(\boldsymbol{v})]_{\boldsymbol{v}\in\mathbb{F}_2^j}$ is given by

$$\boldsymbol{c_j} = H_{2^j}\boldsymbol{d_j} = H_{2^j}\left(\mathbf{1}_{2^j} + (x_l - 1)\,\boldsymbol{e_{2^j}}\right)$$
$$= \boldsymbol{e_1} + \left(\frac{x_l - 1}{2^j}\right)[(-1)^{w_H(\boldsymbol{v})}]^T_{\boldsymbol{v}\in\mathbb{F}_2^j}. \tag{53}$$

The recursive construction for the Walsh-Hadamard matrix leads to a recursion for the coefficients $c_j(\boldsymbol{v})$,

$$\boldsymbol{c_{j+1}} = \frac{1}{2}\begin{bmatrix} H_{2^j} & H_{2^j} \\ H_{2^j} & -H_{2^j}\end{bmatrix}\begin{bmatrix}\mathbf{1}_{2^j}\\ \boldsymbol{d_j}\end{bmatrix} \tag{54}$$

so that

$$c_{j+1}([0,\boldsymbol{v}]) = (e_1)_{\boldsymbol{v}} + \left(\frac{x_l - 1}{2^{j+1}}\right)(-1)^{w_H(\boldsymbol{v})}, \tag{55}$$

and

$$c_{j+1}([1,\boldsymbol{v}]) = -\left(\frac{x_l - 1}{2^{j+1}}\right)(-1)^{w_H(\boldsymbol{v})}. \tag{56}$$

Here $\boldsymbol{e_1} = [(e_1)_{\boldsymbol{v}}]_{\boldsymbol{v}\in\mathbb{F}_2^{2^j}}$. Note that $w_H(\boldsymbol{v}) + w_H(\mathbf{1}_j\oplus\boldsymbol{v}) = j$. If j is odd, then $(-1)^{w_H(\boldsymbol{v})} = -(-1)^{w_H(\mathbf{1}_j\oplus\boldsymbol{v})}$ and

$$c_j(\boldsymbol{v}) = c_{j+1}([0,\boldsymbol{v}]) + c_{j+1}([1,\mathbf{1}_j\oplus\boldsymbol{v}]). \tag{57}$$

Let $\boldsymbol{t} = [0,\ldots,0,1] \in \mathbb{F}_2^j$. If j is even, then $(-1)^{w_H(\boldsymbol{v})} = -(-1)^{w_H(\mathbf{1}_j\oplus\boldsymbol{v}\oplus\boldsymbol{t})}$ and

$$c_j(\boldsymbol{v}) = c_{j+1}([0,\boldsymbol{v}]) + c_{j+1}([1,\mathbf{1}_j\oplus\boldsymbol{v}\oplus\boldsymbol{t}]). \tag{58}$$

Figure 6 describes the splitting process of the cases $j = 1, 2$.

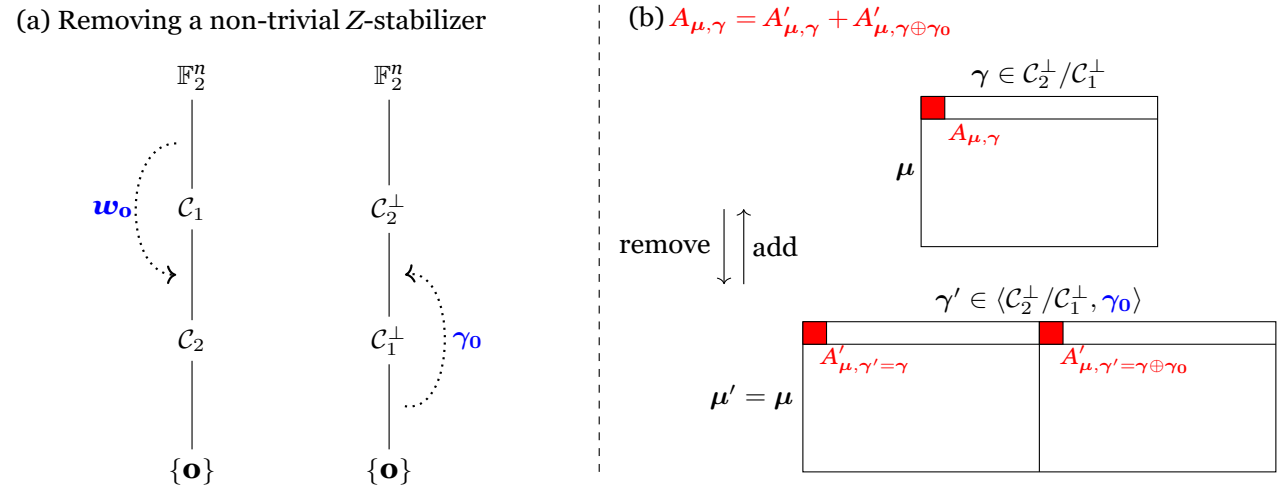

Figure 4 • (**a**) Removing a Z-stabilizer γ_0 creates a new Z-logical, and transforms an old Z-syndrome $\boldsymbol{w_o}$ into a new X-logical. (**b**) Removing/adding a Z-stabilizer induces splitting/grouping of generator coefficients. Graph from [69].

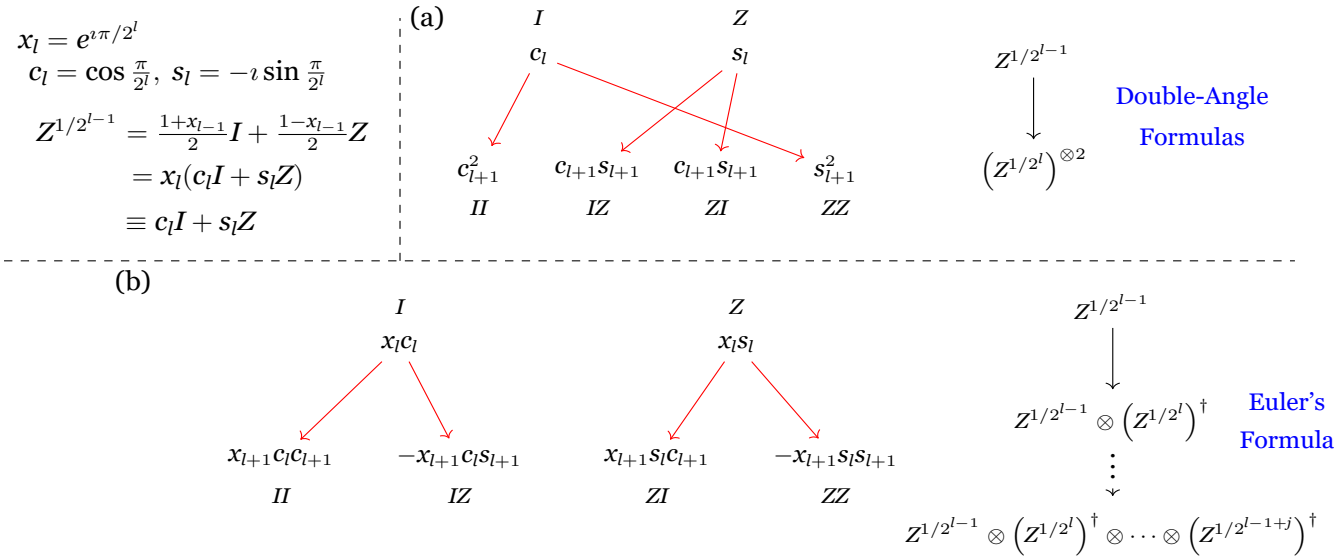

Figure 5 • Admissible Splits of Z-rotations: (**a**) One step for uniform rotations from $Z^{1/2^{l-1}}$ to $Z^{1/2^l} \otimes Z^{1/2^l}$; (**b**) Multi-step for non-uniform rotations $Z \to Z \otimes P^\dagger \to Z \otimes P^\dagger \otimes T^\dagger \to \cdots$. Graph from [69].

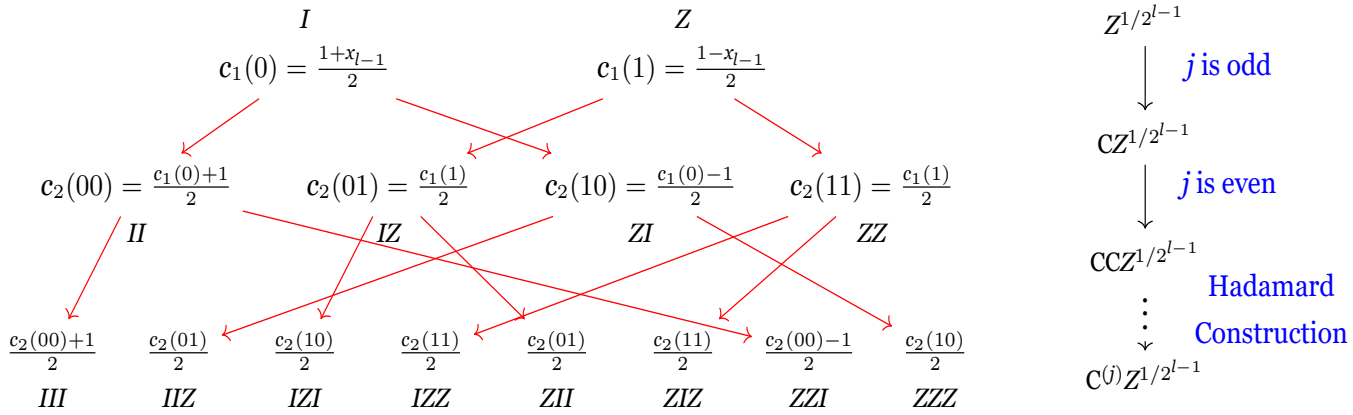

Figure 6 • Admissible Splits from $\mathrm{C}^{(j-1)}Z^{1/2^{l-1}}$ to $\mathrm{C}^{(j)}Z^{1/2^{l-1}}$ for any fixed $l \geq 1$. Graph from [69].

It then follows from **(53)**, **(55)** and **(56)** that the requirement for $s_\gamma(\boldsymbol{w_o})$ is the same as in **(45)**. Although they share the same splitting rule, the global phase x_l they differ becomes a local phase after splitting since $s_{\gamma=\mathbf{o}} = 1 \neq 0$.

Note that the admissible splits we describe include all the elementary operators in the diagonal Clifford hierarchy as shown in **Figure 7**. **Figure 5** corresponds to the vertical line in **Figure 7**, and **Figure 6** corresponds to the oblique line in **Figure 7**.

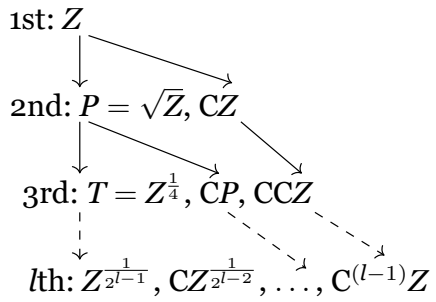

Figure 7 • Admissible splits among the elementary operators in the diagonal Clifford hierarchy. Graph from [69].

We now describe how to choose the new X-logical $\boldsymbol{w_o}$ to lift the level of the induced logical operator. For $l \geq 1$ we suppose that the physical transversal Z-rotation $\left(\exp\left(-\imath\frac{\pi}{2^l}\right)Z\right)^{\otimes n}$ preserves an $[\![n,k,d]\!]$ CSS$(X,\mathcal{C}_2;Z,\mathcal{C}_1^\perp,\boldsymbol{y}=\mathbf{o})$ code, inducing a single $Z^{1/2^{l-1}}$ or $\mathrm{C}^{(j)}Z^{1/2^{l-1}}$.

Theorem 2. *Suppose that after concatenation, the removal of Z-stabilizers introduces the new X-logical $\boldsymbol{w_o} = [\mathbf{1}_n, \mathbf{o}_n]$.*

Then, the logical operator lifts to $\left(Z^{1/2^l}\right)^{\otimes 2}$ or $\mathrm{C}^{(j)}Z^{1/2^{l-1}}$.

Proof. Concatenation transforms the physical operator

$$U_Z = \left(\exp\left(-\imath\frac{\pi}{2^l}Z\right)\right)^{\otimes n} \equiv \left(Z^{1/2^{l-1}}\right)^{\otimes n} \tag{59}$$

into

$$U'_Z = \left(\exp\left(-\imath\frac{\pi}{2^{l+1}}Z\right)\right)^{\otimes 2n} \equiv \left(Z^{1/2^l}\right)^{\otimes 2n}. \tag{60}$$

The physical operator U'_Z preserves the $[\![2n,k,d' \geq d]\!]$ CSS$(X,\mathcal{C}'_2;Z,(\mathcal{C}'_1)^\perp,\boldsymbol{y}' = [\mathbf{o}_n,\mathbf{o}_n])$ codespace, as shown in **Figure 3** and Theorem 1. After concatenation, every element in $\mathcal{C}'_1$ takes the form $[\boldsymbol{u},\boldsymbol{u}]$ for some $\boldsymbol{u} \in \mathcal{C}_1$. Since $\boldsymbol{w_o} = [\mathbf{1}_n,\mathbf{o}_n] \notin \mathcal{C}'_1$, we can introduce $\boldsymbol{w_o}$ as a new X-logical ($\mathcal{C}''_1 = \langle \mathcal{C}'_1, \boldsymbol{w_o}\rangle$). Concatenation does not change the generator coefficients, and it follows from [38] (Lemma 4) that

$$d_{[\boldsymbol{u},\boldsymbol{u}]} = \left(e^{-\imath\frac{\pi}{2^{l+1}}}\right)^{2n-2w_H([\boldsymbol{u},\boldsymbol{u}])} \tag{61}$$

for $[\boldsymbol{u},\boldsymbol{u}] \in \mathcal{C}'_1$. Let $\boldsymbol{\gamma} \in \mathcal{C}_2^\perp/\mathcal{C}_1^\perp$. Then $[\boldsymbol{\gamma},\mathbf{o}] \in (\mathcal{C}'_2)^\perp/(\mathcal{C}'_1)^\perp$, and it follows form **(39)** that

$$\begin{aligned} &s_{[\boldsymbol{\gamma},\mathbf{o}]}([\mathbf{1},\mathbf{o}]) \\ &= \frac{1}{|\mathcal{C}'_1|}\sum_{[\mathbf{1}\oplus\boldsymbol{u},\boldsymbol{u}]\in\mathcal{C}'_1+[\mathbf{1},\mathbf{o}]} (-1)^{[\boldsymbol{\gamma},\mathbf{o}][\mathbf{1}\oplus\boldsymbol{u},\boldsymbol{u}]^T} d_{[\mathbf{1}\oplus\boldsymbol{u},\boldsymbol{u}]\oplus[\mathbf{o},\mathbf{o}]} \\ &= \frac{1}{|\mathcal{C}_1|}\sum_{\boldsymbol{u}\in\mathcal{C}_1} (-1)^{\boldsymbol{\gamma}(\mathbf{1}\oplus\boldsymbol{u})^T}\left(e^{-\imath\frac{\pi}{2^{l+1}}}\right)^{2n-2w_H([\mathbf{1}\oplus\boldsymbol{u},\boldsymbol{u}])}. \end{aligned} \tag{62}$$

Since $w_H([\mathbf{1}\oplus\boldsymbol{u},\boldsymbol{u}]) = n$ for all $\boldsymbol{u} \in \mathcal{C}_1$, we have

$$\begin{aligned} s_{[\boldsymbol{\gamma},\mathbf{o}]}([\mathbf{1},\mathbf{o}]) &= (-1)^{\boldsymbol{\gamma}\mathbf{1}^T}\frac{1}{|\mathcal{C}_1|}\sum_{\boldsymbol{u}\in\mathcal{C}_1}(-1)^{\boldsymbol{\gamma}\boldsymbol{u}^T} \\ &= \begin{cases} 1, & \text{if } \boldsymbol{\gamma} = \mathbf{o}, \\ 0, & \text{if } \boldsymbol{\gamma} \neq \mathbf{o}, \end{cases} \end{aligned} \tag{63}$$

and the theorem now follows from **(45)**. □

Example 3. (Continued: from $[\![14,1,3]\!]$ to $[\![14,2,2]\!]$; Logical $P^\dagger \to (T^\dagger)^{\otimes 2}$). *The $[\![14,1,3]\!]$ code is obtained by concatenating the $[\![7,1,3]\!]$ Steane code. We introduce the new X-logical $\boldsymbol{w_o} = [\mathbf{1},\mathbf{0}] \in \mathbb{F}_2^{2n}$ by removing the Z-stabilizer $\boldsymbol{\gamma_0} = [\mathbf{1},\mathbf{1}] \in (\mathcal{C}'_1)^\perp$ to produce the $[\![14,2,2]\!]$ code. The generator coefficients $A''_{\mathbf{o},\boldsymbol{\gamma}''}\left(\frac{\pi}{4}\right)$ of the $[\![14,2,2]\!]$ code for $\boldsymbol{\gamma}'' \in \langle\boldsymbol{\gamma_1} = [\mathbf{1},\mathbf{0}],\boldsymbol{\gamma_0}\rangle$ under the physical $T^{\otimes 14}$ gate are*

$$\begin{aligned} A''_{\mathbf{o},\boldsymbol{\gamma}''=\mathbf{o}}\left(\frac{\pi}{4}\right) &= \frac{1}{2}\left(\cos\frac{\pi}{4}+1\right) = \left(\cos\frac{\pi}{8}\right)^2, \\ A''_{\mathbf{o},\boldsymbol{\gamma}''=\boldsymbol{\gamma_1}}\left(\frac{\pi}{4}\right) &= \frac{1}{2}\imath\sin\frac{\pi}{4} = \imath\sin\frac{\pi}{8}\cos\frac{\pi}{8}. \end{aligned} \tag{64}$$

Splitting gives

$$\begin{aligned} A''_{\mathbf{o},\boldsymbol{\gamma}''=\boldsymbol{\gamma_0}} &= A'_{\mathbf{o},\mathbf{o}} - A''_{\mathbf{o},\boldsymbol{\gamma}''=\mathbf{o}} = \left(\imath\sin\frac{\pi}{8}\right)^2, \\ A''_{\mathbf{o},\boldsymbol{\gamma}''=\boldsymbol{\gamma_1}\oplus\boldsymbol{\gamma_0}} &= A'_{\mathbf{o},\boldsymbol{\gamma_1}} - A''_{\mathbf{o},\boldsymbol{\gamma}''=\boldsymbol{\gamma_1}} = \imath\sin\frac{\pi}{8}\cos\frac{\pi}{8}. \end{aligned} \tag{65}$$

*It follows from **(21)** that the logical operator induced by $T^{\otimes 14}$ on the $[\![14,2,2]\!]$ codespace is $\left(T^\dagger\right)^{\otimes 2}$. Note that the $[\![14,2,2]\!]$ code is a member of the triorthogonal code family introduced by Bravyi and Haah [26]. The operations described above can transform the $[\![15,1,3]\!]$ triorthogonal code [24, 29, 72, 73] to the $[\![30,2,2]\!]$ code for which the physical transversal $\sqrt{T}$ induces a logical $\sqrt{T}^\dagger$. The same operations work for the whole punctured Reed–Muller family $[\![2^{l+1}-1,1,3]\!]$ [29] that realizes the single logical $Z^{1/2^{l-1}} \in \mathcal{C}_d^{(l)}$ and results in the $[\![2^{l+2}-2,2,2]\!]$ triorthogonal code family realizing the logical transversal $Z^{1/2^l} \in \mathcal{C}_d^{(l+1)}$.*

Example 4. (Continued: the $[\![2^l,l,2]\!]$ code family realizes $\mathrm{C}^{(l-1)}Z$). *Starting from the $[\![4,2,2]\!]$ code, we first concatenate to obtain the $[\![8,2,2]\!]$ code and then remove the Z-stabilizer associated with adding the new X-logical $\boldsymbol{w_o} = [\mathbf{1},\mathbf{0}]$ to produce the $[\![8,3,2]\!]$ code. The $[\![4,2,2]\!]$ code realizes $C^{(1)}Z$ = CZ up to some logical Pauli Z by either physical transversal Phase gate $P^{\otimes 4}$ or transversal Control-Z gate $CZ^{\otimes 2}$. The $[\![8,3,2]\!]$ code realizes $C^{(2)}Z$ = CCZ up to some logical Pauli Z by either physical transversal T gate $T^{\otimes 8}$ or transversal Control-Phase gate $CP^{\otimes 4}$. Repeated concatenation and removal of Z-stabilizers yields the $[\![2^l,l,2]\!]$ code family that supports the logical $C^{(l-1)}Z$ gate up to some logical Pauli Z. When the physical gate is a transversal Z-rotation, the generator coefficients of the $[\![2^l,l,2]\!]$ code family are listed in **Table 1** below.*

Table 1 • The Splitting of generator coefficients for the induced logical $\mathrm{C}^{(l-1)}\mathrm{Z}$ (up to some logical Pauli Z). The $[\![2^l,l,2]\!]$ CSS codes are preserved by physical transversal Z-rotations $\left(\exp\left(-\imath\frac{\pi}{2^{l-1}}Z\right)\right)^{\otimes 2^l}$. Table from [69].

	U_Z^L up to Z^L	Generator coefficients $A_{\mathbf{o},\boldsymbol{\gamma}}$
2	$\mathrm{C}^{(1)}Z$	$\frac{1}{2}\ -\frac{1}{2}\ -\frac{1}{2}\ -\frac{1}{2}$
3	$\mathrm{C}^{(2)}Z$	$\frac{3}{4}\ -\frac{1}{4}\ -\frac{1}{4}\ \cdots\ -\frac{1}{4}\ -\frac{1}{4}$
l	$\mathrm{C}^{(l-1)}\mathrm{Z}$	$\frac{2^{l-1}-1}{2^{l-1}}\ -\frac{1}{2^{l-1}}\ -\frac{1}{2^{l-1}}\ \cdots\ -\frac{1}{2^{l-1}}$

Since removing Z-stabilizers may decrease code distance, we introduce a third elementary operation in the next Section with the aim of increasing the distance.

3.3. Increase distance

Our focus on diagonal gates U_Z that preserve CSS$(X, \mathcal{C}_2; Z, \mathcal{C}_1^\perp, \boldsymbol{y})$ codes implies that the effective distance is the Z-distance, $d_Z = \min_{\boldsymbol{z}\in\mathcal{C}_2^\perp\setminus\mathcal{C}_1^\perp} w_H(\boldsymbol{z})$. Concatenation, described in **Figure 3**, does not change d_Z. Removal of Z-stabilizers increases the number of Z-logicals in $\mathcal{C}_2^\perp \setminus \mathcal{C}_1^\perp$, and this may decrease d_Z. After removing Z-stabilizers, we may need to increase effective distance by introducing new X-stabilizers. We now examine how generator coefficients evolve when we add or remove X-stabilizers.

Adding a new X-stabilizer $\boldsymbol{x_0} \in \mathcal{C}_1 \setminus \mathcal{C}_2$ transforms a CSS(X, $\mathcal{C}_2$; Z, $\mathcal{C}_1^\perp$, $\boldsymbol{y}$) code to a CSS(X, $\langle\mathcal{C}_2, \boldsymbol{x_0}\rangle$; Z, $\mathcal{C}_1^\perp, \boldsymbol{y}$) code. A Z-logical $\boldsymbol{\mu_0}$ in the original code becomes an X-syndrome in the new code. Note that $\boldsymbol{\mu_0} \in \mathcal{C}_2^\perp \setminus \mathcal{C}_1^\perp$ and $\boldsymbol{\mu_0} \notin \langle\mathcal{C}_2, \boldsymbol{x_0}\rangle^\perp \setminus \mathcal{C}_1^\perp$. The number of Z-logicals is halved, while the number of X-syndromes is doubled, so the number of generator coefficients remains constant. Let U_Z be a fixed diagonal physical gate. The generator coefficients $A_{\boldsymbol{\mu},\boldsymbol{\gamma}}$ for the old code determine the generator coefficients $A'_{\boldsymbol{\mu}',\boldsymbol{\gamma}'}$ for the new code as follows:

$$A'_{\boldsymbol{\mu}',\boldsymbol{\gamma}'} = \sum_{\boldsymbol{z}\in\mathcal{C}_1^\perp+\boldsymbol{\mu}'+\boldsymbol{\gamma}'} \epsilon_{(\mathbf{o},\boldsymbol{z})} f(\boldsymbol{z}) = \begin{cases} A_{\boldsymbol{\mu}',\boldsymbol{\gamma}'}, & \text{if } \boldsymbol{\mu}' \in \mathbb{F}_2^n/\mathcal{C}_2^\perp, \\ A_{\boldsymbol{\mu}'\oplus\boldsymbol{\mu_0},\boldsymbol{\gamma}'\oplus\boldsymbol{\mu_0}}, & \text{if } \boldsymbol{\mu}' \oplus \boldsymbol{\mu_0} \in \mathbb{F}_2^n/\mathcal{C}_2^\perp. \end{cases} \tag{66}$$

Note that the new Z-logical $\boldsymbol{\gamma}' \in \langle\mathcal{C}_2, \boldsymbol{x_0}\rangle^\perp/\mathcal{C}_1^\perp$. If $\boldsymbol{\mu}'$ coincides with an old syndrome, then $A'_{\boldsymbol{\mu}',\boldsymbol{\gamma}'} = A_{\boldsymbol{\mu}',\boldsymbol{\gamma}'}$. Otherwise $\boldsymbol{\mu}' \oplus \boldsymbol{\mu_0} \in \mathbb{F}_2^n/\mathcal{C}_2^\perp$ and $\boldsymbol{\gamma}' \oplus \boldsymbol{\mu_0} \in \mathcal{C}_2^\perp/\mathcal{C}_1^\perp$. **Figure 8** captures the process of adding and removing X-stabilizers. Note that **(66)** is reversed when an X-stabilizer is removed.

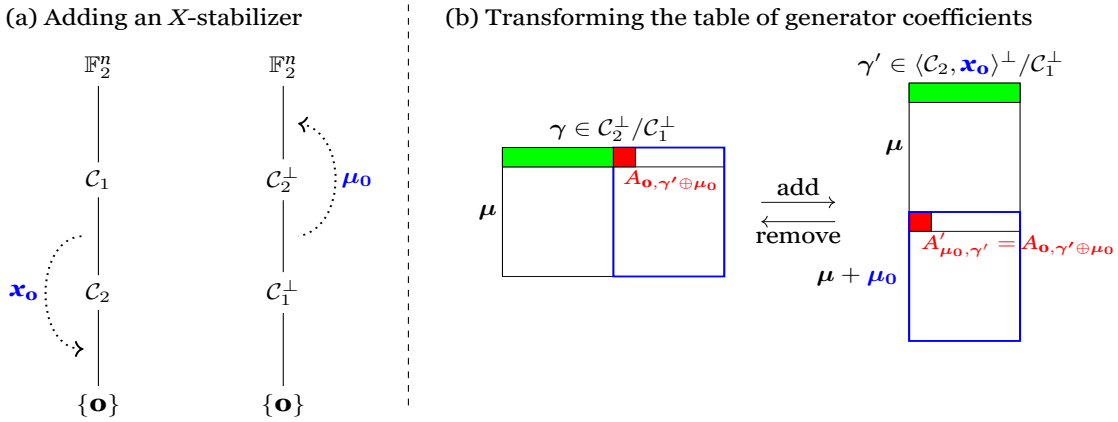

Figure 8 • (**a**) Adding the old X-logical $\boldsymbol{x_0}$ as a new X-stabilizer transforms the old Z-logical μ_0 to a new X-syndrome. (**b**) Introducing a new X-stabilizer $\boldsymbol{x_0}$ doubles the number of X-syndromes and halves the number of Z-logicals. The blue rectangle shifts as the generator coefficients evolve. Graph from [69].

If we remove an X-stabilizer from a CSS code that is preserved by a diagonal gate U_Z, then the new code is still preserved by U_Z. If instead, we add an X-stabilizer, then the new code may fail to be preserved by U_Z. We say that the addition of an X-stabilizer is *admissible* if the new code is preserved by U_Z. We now characterize admissible additions in terms of the new X-syndrome $\boldsymbol{\mu_0}$.

Let $\mathcal{C}_2^\perp/\mathcal{C}_1^\perp = \langle D, \boldsymbol{\mu_0}\rangle$. The old is preserved by U_Z if and only if

$$\sum_{\boldsymbol{\gamma}\in\langle D,\boldsymbol{\mu_0}\rangle} |A_{\mathbf{o},\boldsymbol{\gamma}}|^2 = 1, \tag{67}$$

and the new code is preserved by U_Z if and only if

$$\sum_{\boldsymbol{\gamma}\in D} |A_{\mathbf{o},\boldsymbol{\gamma}}|^2 = 1. \tag{68}$$

Addition of $\boldsymbol{x_0}$ is admissible if and only if

$$A_{\mathbf{o},\boldsymbol{\gamma}} = 0 \text{ for all } \boldsymbol{\gamma} \in D + \boldsymbol{\mu_0}. \tag{69}$$

We require that half the generator coefficients $A_{\mathbf{o},\boldsymbol{\gamma}}$ vanish. The non-vanishing coefficients appear in the green rectangle shown in **Figure 8b**. Then, it follows from **(21)** that the logical operator stays at the same level after an admissible addition. It also follows from **(40)** and **(41)** that an addition is admissible if and only if

$$s_{\boldsymbol{\gamma}}(\boldsymbol{w_0}) = \pm A_{\mathbf{o},\boldsymbol{\gamma}} \text{for all} \boldsymbol{\gamma} \in \mathcal{C}_2^\perp/\mathcal{C}_1^\perp. \tag{70}$$

We may need to concatenate several times and remove several independent Z-stabilizers to create enough zeros among the generator coefficients.

We now combine concatenation, removal of Z-stabilizers, and addition of X-stabilizers to construct a CSS code family with growing distance that is preserved by diagonal operators with increasing logical level in the Clifford hierarchy.

Example 5. (Quantum Reed–Muller (QRM) Code Family). *Introduced in [38] (Theorem 14) and [41] (Theorem 19), this is a family of* $[\![2^m, \binom{m}{r}, 2^{\min\{r,m-r\}}]\!]$ *CSS codes preserved by physical transversal* Z*-rotations* $\left(Z^{1/2^{(m/r-1)}}\right)^{\otimes 2^m}$ *when* $r \mid m$. *We now describe how these codes are constructed by concatenation followed by removal of* Z*-stabilizers and addition of* X*-stabilizers.*

Let $r \geq 1$ *be fixed. Note that* m/r *increases by* 1 *when* m *increases by* r*, and that the new code is preserved by a physical gate that is one level higher in the Clifford hierarchy. We start from a* $[\![2^m, \binom{m}{r}, 2^{\min\{r,m-r\}}]\!]$ *CSS code determined by* $\mathcal{C}_1 = \mathrm{RM}(r, m)$ *and* $\mathcal{C}_2 = \mathrm{RM}(r-1, m)$. *The recursive construction of classical*

Reed–Muller codes [74] is given by

$$\mathrm{RM}(r, m+1) = \{(\boldsymbol{u}, \boldsymbol{u} \oplus \boldsymbol{v}) \,|\boldsymbol{u} \in \mathrm{RM}(r, m), \\ \boldsymbol{v} \in \mathrm{RM}(r-1, m)\}. \quad (71)$$

Let $\mathbf{1}_{2^r}$ denotes the vector of length 2^r with every entry equals to 1. We concatenate our CSS code r times to construct the $[\![2^{m+r}, \binom{m}{r}, 2^{\min\{r,m-r\}}]\!]$ CSS code determined by $\mathcal{C}_1' = \mathbf{1}_{2^r} \otimes \mathrm{RM}(r, m)$ and $\mathcal{C}_2' = \mathbf{1}_{2^r} \otimes \mathrm{RM}(r-1, m)$. Note that $\mathcal{C}_1' \subseteq \mathrm{RM}(r, m+r)$ and $\mathcal{C}_2' \subseteq \mathrm{RM}(r-1, m+r)$. We now remove the Z-stabilizers and add the X-stabilizers to make $\mathcal{C}_1' = \mathrm{RM}(r, m+r)$, $\mathcal{C}_2' = \mathrm{RM}(r-1, m+r)$. We obtain the $[\![2^{m+r}, \binom{m+r}{r}, 2^{\min\{r,m\}}]\!]$ CSS code, which is the next member of the QRM code family. The level of the new induced logical operator equals that of the new physical transversal Z-rotations [41] (Theorem 19), which is one level higher than that of the old induced logical operator. For fixed r, the operations described above just maintain the distance.

*To achieve the growing distance, we can increase r by 1 and increase m by $h := r + \frac{m}{r} + 1$ so that $\frac{m}{r} + 1 = \frac{m+h}{r+1}$. When $r \mid m$, it follows from **(71)** that we can obtain the $[\![2^{m+h}, \binom{m+h}{r+1}, 2^{\min\{r+1, m+h-r-1\}}]\!]$ CSS code from a $[\![2^m, \binom{m}{r}, 2^{\min\{r,m-r\}}]\!]$ CSS code by first concatenating h times, then removing $\left(\binom{m+h}{r+1} + \binom{m+h}{r} - \binom{m}{r}\right)$ Z-stabilizers, and adding $\binom{m+h}{r}$ X-stabilizers. The logical operator induced by the new code is one level higher than that of the old code, and the distance doubles for the new code. **Figure 1** illustrates the case when $m = 2$ and $r = 1$.*

4. Discussion

Given a CSS code that realizes a diagonal gate at the l^{th} level, we have introduced three basic operations that can be combined to construct a new CSS code that realizes a diagonal gate at the $(l+1)^{\text{th}}$ level in the Clifford hierarchy. The three basic operations are concatenation (to increase the physical level), removal of *Z*-stabilizers (to increase the logical level and increase code rate), and addition of *X*-stabilizers (to increase the distance). We have derived necessary and sufficient conditions for admissibility, that is, for the new code to be preserved by the target physical operator. We have described these conditions using the mathematical framework of generator coefficients. Concatenation is always admissible, while the other two basic operations may not be admissible. We have demonstrated the power of combining the three basic operations to synthesize a target diagonal operator by climbing the Clifford hierarchy to construct the QRM code family.

In future work, we expect to explore how best to balance removal of *Z*-stabilizers and addition of *X*-stabilizers. We will also investigate the existence of code families corresponding to **Figure 5b**.

Acknowledgments

The authors would like to thank Ken Brown's group for helpful discussions. J.H. and Q.L. started this work during their Ph.D. studies in Mathematics at Duke University (graduated 2023), and continued to develop it thereafter.

Funding

This research was sponsored by the National Science Foundation under grants 1908730, 2106213 and 2120757.

Author contributions

Conceptualization, methodology, and validation, J.H., Q.L. and R.C.; writing—original draft, J.H. and Q.L.; writing—review and editing, R.C.; funding acquisition, R.C. All authors have read and agreed to the published version of the manuscript.

Conflict of interest

The authors declare that they have no competing interests.

Data availability statement

All data supporting the findings of this publication are available within this article.

Additional information

Received: 2025-06-20

Accepted: 2025-10-09

Published: 2025-10-21

Academia Quantum papers should be cited as *Academia Quantum 2025*, ISSN 3064-979X, https://doi.org/10.20935/AcadQuant7957. The journal's official abbreviation is *Acad. Quant.*

Publisher's note

Academia.edu Journals stays neutral with regard to jurisdictional claims in published maps and institutional affiliations. All claims expressed in this article are solely those of the authors and do not necessarily represent those of their affiliated organizations, or those of the publisher, the editors and the reviewers. Any product that may be evaluated in this article, or claim that may be made by its manufacturer, is not guaranteed or endorsed by the publisher.

Copyright

© 2025 copyright by the authors. This article is an open access article distributed under the terms and conditions of the Creative Commons Attribution (CC BY) license (https://creativecommons.org/licenses/by/4.0/).

References

1. Calderbank RA, Shor PW. Good quantum error-correcting codes exist. Phys Rev A. 1996;54:1098–105. doi: 10.1103/physreva.54.1098

2. Steane AM. Simple quantum error-correcting codes. Phys Rev A. 1996;54(6):4741–51. doi: 10.1103/PhysRevA.54.4741

3. Gottesman D. Stabilizer codes and quantum error correction. Pasadena (CA): California Institute of Technology; 1997. doi: 10.48550/arXiv.quant-ph/9705052

4. Calderbank RA, Rains EM, Shor PW, Sloane NJA. Quantum error correction via codes over *GF*(4). IEEE Trans Inf Theory. 1998;44(4):1369–87. doi: 10.1109/isit.1997.613213

5. Nielsen MA, Chuang IL. Quantum computation and quantum information: 10th anniversary edition. Cambridge: Cambridge University Press; 2011. ISBN 1107002176.

6. Preskill J. Quantum computing in the NISQ era and beyond. Quantum. 2018;2:79. doi: 10.22331/q-2018-08-06-79

7. Iverson JK, Preskill J. Coherence in logical quantum channels. New J Phys. 2020;22(7):073066. doi: 10.1088/1367-2630/ab8e5c

8. Walter T, Kurpiers P, Gasparinetti S, Magnard P, Potočnik A, Salathé Y, et al. Rapid high-fidelity single-shot dispersive readout of superconducting qubits. Phys Rev Appl. 2017;7:054020. doi: 10.1103/PhysRevApplied.7.054020

9. Fang C, Wang Y, Huang S, Brown KR, Kim J. Crosstalk suppression in individually addressed two-qubit gates in a trapped-ion quantum computer. Phys Rev Lett. 2022;129(24):240504. doi: 10.1103/physrevlett.129.240504

10. Boykin PO, Mor T, Pulver M, Roychowdhury V, Vatan F. On universal and fault-tolerant quantum computing: a novel basis and a new constructive proof of universality for shor's basis. Proceedings of the 40th Annual Symposium on Foundations of Computer Science (Cat. No. 99CB37039); 1999 Oct 17–19; New York, NY, USA. 1999. p. 486–94. doi: 10.1109/sffcs.1999.814621

11. Gottesman D, Chuang IL. Demonstrating the viability of universal quantum computation using teleportation and single-qubit operations. Nature. 1999;402(6760):390–3. doi: 10.1038/46503

12. Zeng B, Chen X, Chuang IL. Semi-clifford operations, structure of C_k hierarchy, and gate complexity for fault-tolerant quantum computation. Phys Rev A. 2008;77(4):042313. doi: 10.1103/physreva.77.042313

13. Beigi S, Shor PW. C_3, semi-clifford and generalized semi-clifford operations. Quantum Inf Comput. 2010;10(1&2):41–59. doi: 10.26421/QIC10.1-2-4

14. Bengtsson I, Blanchfield K, Campbell ET, Howard M. Order 3 symmetry in the clifford hierarchy. J Phys A Math Theor. 2014;47(45):455302. doi: 10.1088/1751-8113/47/45/455302

15. Cui SX, Gottesman D, Krishna A. Diagonal gates in the clifford hierarchy. Phys Rev A. 2017;95(1):012329. doi: 10.1103/physreva.95.012329

16. Rengaswamy N, Calderbank RA, Pfister HD. Unifying the clifford hierarchy via symmetric matrices over rings. Phys Rev A. 2019;100(2):022304. doi: 10.1103/physreva.100.022304

17. Pllaha T, Rengaswamy N, Tirkkonen O, Calderbank RA. Unweyl-ing the clifford hierarchy. Quantum. 2020;4:370. doi: 10.22331/q-2020-12-11-370

18. Anderson JT. On groups in the qubit clifford hierarchy. Quantum. 2024;8:1370. doi: 10.22331/q-2024-06-13-1370

19. He Z, Robitaille L, Tan X. Permutation gates in the third level of the clifford hierarchy. arXiv. 2024;arXiv:2410.11818. doi: 10.48550/arXiv.2410.11818

20. Metger T, Poremba A, Sinha M, Yuen H. Simple Constructions of Linear-Depth t-Designs and Pseudorandom Unitaries. Proceedings of the 2024 IEEE 65th Annual Symposium on Foundations of Computer Science (FOCS); 2024 Oct 27–30; Chicago, IL, USA. 2024. p. 485–92. doi: 10.1109/FOCS61266.2024.00038

21. Chen CF, Haah J, Haferkamp J, Liu Y, Metger T, Tan X. Incompressibility and spectral gaps of random circuits. arXiv. 2024; arXiv:2406.07478. doi: 10.48550/arXiv.2406.07478

22. Shor PW. Algorithms for quantum computation: discrete logarithms and factoring. Proceedings of the 35th Annual Symposium on Foundations of Computer Science Pages; 1994 Nov 20–22; Santa Fe, NM, USA. 1994. p. 124–34. doi: 10.1109/SFCS.1994.365700

23. Shor PW. Polynomial-time algorithms for prime factorization and discrete logarithms on a quantum computer. SIAM Rev. 1999;41(2):303–32. doi: 10.1137/S0036144598347011

24. Bravyi S, Kitaev A. Universal quantum computation with ideal clifford gates and noisy ancillas. Phys Rev A. 2005;71(2):022316. doi: 10.1103/physreva.71.022316

25. Reichardt BW. Quantum universality from magic states distillation applied to CSS codes. Quantum Inf Process. 2005;4(3):251–64. doi: 10.1007/s11128-005-7654-8

26. Bravyi S, Haah J. Magic-state distillation with low overhead. Phys Rev A. 2012;86(5):052329. doi: 10.1103/physreva.86.052329

27. Anwar H, Campbell ET, Browne DE. Qutrit magic state distillation. New J Phys. 2012;14(6):063006. doi: 10.1088/1367-2630/14/6/063006

28. Campbell ET, Anwar H, Browne DE. Magic-state distillation in all prime dimensions using quantum reed-muller codes. Phys Rev X. 2012;2(4):041021. doi: 10.1103/physrevx.2.041021

29. Landahl AJ, Cesare C. Complex instruction set computing architecture for performing accurate quantum *z* rotations with less magic. arXiv. 2013;arXiv:1302.3240. doi: 10.48550/arXiv.1302.3240

30. Campbell ET, Howard M. Unified framework for magic state distillation and multiqubit gate synthesis with reduced resource cost. Phys Rev A. 2017;95(2):022316. doi: 10.1103/physreva.95.022316

31. Haah J, Hastings MB. Codes and protocols for distilling T, controlled-S, and toffoli gates. Quantum. 2018;2:71. doi: 10.22331/q-2018-06-07-71

32. Krishna A, Tillich JP. Towards low overhead magic state distillation. Phys Rev Lett. 2019;123(7):070507. doi: 10.1103/physrevlett.123.070507

33. Vuillot C, Breuckmann NP. Quantum pin codes. IEEE Trans Inf Theory. 2022;68(9):5955–74. doi: 10.1109/tit.2022.3170846

34. Wills A, Hsieh M, Yamasaki H. Constant-overhead magic state distillation. arXiv. 2024;arXiv:2408.07764. doi: 10.48550/arXiv.2408.07764

35. Gidney C, Shutty N, Jones C. Magic state cultivation: growing T states as cheap as cnot gates. arXiv. 2024;arXiv:2409.17595. doi: 10.48550/arXiv.2409.17595

36. Itogawa T, Takada Y, Hirano Y, Fujii K. Efficient magic state distillation by zero-level distillation distillation. arXiv. 2024;arXiv:2403.03991. doi: 10.48550/arXiv.2403.03991

37. Lee S, Thomsen F, Fazio N, Brown BJ, Bartlett SD. Low-overhead magic state distillation with color codes. arXiv. 2025;arXiv:2409.07707. doi: 10.48550/arXiv.2409.07707

38. Hu J, Liang Q, Calderbank R. Designing the quantum channels induced by diagonal gates. Quantum. 2022;6:802. doi: 10.22331/q-2022-09-08-802

39. Hu J, Liang Q, Calderbank R. Co-design of CSS codes and diagonal gates. Proceedings of the 2022 IEEE International Symposium on Information Theory (ISIT); 2022 Jun 26–Jul 1; Espoo, Finland; 2022. p. 1229–34.

40. Haah J. Towers of generalized divisible quantum codes. Phys Rev A. 2018;97(4):042327. doi: 10.1103/PhysRevA.97.042327

41. Rengaswamy N, Calderbank RA, Newman M, Pfister HD. On optimality of CSS codes for transversal *T*. IEEE J Sel Areas Inf Theory. 2020;1(2):499–514. doi: 10.1109/jsait.2020.3012914

42. Camps-Moreno E, López HH, Matthews GL, Ruano D, San-José R, Soprunov I. An algebraic characterization of binary CSS-T codes and cyclic CSS-T codes for quantum fault tolerance. Quantum Inf Process. 2024;23(6):230. doi: 10.1007/s11128-024-04427-5

43. Camps-Moreno E, Lopez HH, Matthews GL, McMillon E. Toward quantum CSS-T codes from sparse matrices. arXiv. 2024;arXiv:2406.00425. doi: 10.48550/arXiv.2406.00425

44. Berardini E, Caminata A, Ravagnani A. Structure of CSS and CSS-T quantum codes. Des Codes Cryptogr. 2024;92(10):2801–23. doi: 10.1007/s10623-024-01415-9

45. Berardini E, Dastbasteh R, Martinez JE, Jain S, Larrarte OS. Asymptotically good CSS-T codes exist. arXiv. 2024;arXiv:2412.08586. doi: 10.48550/arXiv.2412.08586

46. Andrade E, Bolkema J, Dexter T, Eggers H, Luongo V, Manganiello F, et al. CSS-T codes from reed muller codes. arXiv. 2025;arXiv:2305.06423. doi: 10.48550/arXiv.2305.06423

47. Anderson JT, Weippert M. Controlled gates in the clifford hierarchy. arXiv. 2025;arXiv:2410.04711. doi: 10.48550/arXiv.2410.04711

48. Barg A, Coble NJ, Hangleiter D, Kang C. Geometric structure and transversal logic of quantum reed-muller codes. arXiv. 2024;arXiv:2410.07595. doi: 10.48550/arXiv.2410.07595

49. Beale SJ, Wallman JJ, Gutiérrez M, Brown KR, Laflamme R. Quantum error correction decoheres noise. Phys Rev Lett. 2018;121(19):190501. doi: 10.1103/PhysRevLett.121.190501

50. Huang E, Doherty AC, Flammia S. Performance of quantum error correction with coherent errors. Phys Rev A. 2019;99(2):022313. doi: 10.1103/PhysRevA.99.022313

51. Pato B, Staples JW, Brown KR. Logical coherence in two-dimensional compass codes. Phys Rev A. 2025;111:032424. doi: 10.1103/PhysRevA.111.032424

52. Hu J, Liang Q, Rengaswamy N, Calderbank R. Mitigating coherent noise by balancing weight-2 *Z*-stabilizers. IEEE Trans Inf Theory. 2022;68(3):1795–808. doi: 10.1109/tit.2021.3130155

53. Debroy DM, Egan L, Noel C, Risinger A, Zhu D, Biswas D, et al. Optimizing stabilizer parities for improved logical qubit memories. Phys Rev Lett. 2021;127(24):240501. doi: 10.1103/physrevlett.127.240501

54. Cai Z, Xu X, Benjamin SC. Mitigating coherent noise using pauli conjugation. NPJ Quantum Inf. 2020;6(1):17. doi: 10.1038/s41534-019-0233-0

55. Ouyang Y. Avoiding coherent errors with rotated concatenated stabilizer codes. NPJ Quantum Inf. 2021;7(1):87. doi: 10.1038/s41534-021-00429-8

56. Lidar DA, Chuang IL, Whaley KB. Decoherence-free subspaces for quantum computation. Phys Rev.Lett. 1998;81:2594–7. doi: 10.1103/PhysRevLett.81.2594

57. Kempe J, Bacon D, Lidar DA, Whaley KB. Theory of decoherence-free fault-tolerant universal quantum computation. Phys Rev A. 2001;63:042307. doi: 10.1103/PhysRevA.63.042307

58. Alber G, Beth T, Charnes C, Delgado A, Grassl M, Mussinger M. Stabilizing distinguishable qubits against spontaneous decay by detected-jump correcting quantum codes. Phys Rev Lett. 2001;86:4402–5. doi: 10.1103/PhysRevLett.86.4402

59. Pereira FRF, Mancini S, Guardia GGL. Stabilizer codes for open quantum systems. Sci Rep. 2023;13(1):10540. doi: 10.1038/s41598-023-37434-0

60. Dasu S, Criger B, Foltz C, Gerber JA, Gilbreth CN, Gilmore K, et al. Order-of-magnitude extension of qubit lifetimes with a decoherence-free subspace quantum error correction code. arXiv. 2025;arXiv:2503.22107. doi: 10.48550/arXiv.2503.22107

61. Paetznick A, da Silva MP, Ryan-Anderson C, Bello-Rivas JM, Campora JP III, Chernoguzov A, et al. Demonstration of logical qubits and repeated error correction with better-than-physical error rates. arXiv, 2024;arXiv:2404.02280. doi: 10.48550/arXiv.2404.02280

62. Ryan-Anderson C, Brown NC, Baldwin CH, Dreiling JM, Foltz C, Gaebler JP, et al. High-fidelity teleportation of a logical qubit using transversal gates and lattice surgery. arXiv. 2024;arXiv.2404.16728. doi: 10.48550/arXiv.2404.16728

63. Laflamme R, Miquel C, Paz JP, Zurek WH. Perfect quantum error correcting code. Phys Rev Lett. 1996;77:198–201. doi: 10.1103/PhysRevLett.77.198

64. Golowich L, Guruswami V. Asymptotically good quantum codes with transversal non-clifford gates. arXiv. 2024;arXiv:2408.09254. doi: 10.48550/arXiv.2408.09254

65. Jain SP, Albert VV. Transversal clifford and t-gate codes of short length and high distance. IEEE J Sel Areas Inf Theory. 2025;6:127–37. doi: 10.1109/jsait.2025.3570832

66. Vasmer M, Kubica A. Morphing quantum codes. PRX Quantum. 2022;3(3):030319. doi: 10.1103/prxquantum.3.030319

67. Webster MA, Brown BJ, Bartlett SD. The XP stabiliser formalism: a generalisation of the pauli stabiliser formalism with arbitrary phases. Quantum. 2022;6:815. doi: 10.22331/q-2022-09-22-815

68. Webster MA, Quintavalle AO, Bartlett SD. Transversal diagonal logical operators for stabiliser codes. New J Phys. 2023;25(10):103018. doi: 10.1088/1367-2630/acfc5f

69. Hu J. Designing quantum channels induced by diagonal gates [Ph.D. thesis]. Durham (NC): Duke University; 2023 [accessed on 2025 Oct 5]. Available from: https://hdl.handle.net/10161/27636

70. Steane A. Multiple-particle interference and quantum error correction. Proc R Soc Lond A Math Phys Sci. 1996;452(1954):2551–77. doi: 10.1098/rspa.1996.0136

71. Liang Q. Mitigating coherent noise [Ph.D. thesis]. Durham (NC): Duke University; 2023 [accessed on 2025 Oct 5]. Available from: https://hdl.handle.net/10161/27638

72. Knill E, Laflamme R, Zurek W. Threshold accuracy for quantum computation. arXiv. 1996;arXiv:quant-ph/9610011. doi: 10.48550/arXiv.quant-ph/9610011

73. Anderson JT, Duclos-Cianci G, Poulin D. Fault-tolerant conversion between the steane and reed-muller quantum codes. Phys Rev Lett. 2014;113(8):080501. doi: 10.1103/PhysRevLett.113.080501

74. MacWilliams FJ, Sloane NJA. The theory of error correcting codes. Vol 16. Amsterdam: Elsevier; 1977.